People's Democratic Republic of Algeria
Ministry of Higher Education and Scientific Research

University M'Hamed BOUGARA – Boumerdes

Institute of Electrical and Electronic Engineering

Department of Electronics

Final Year Project Report Presented in Partial Fulfilment of the Requirements for the Degree of

MASTER

In **Electrical and Electronic Engineering**

Option: **Computer Engineering**

Title:

QRS Detection in ECG Signals

Presented by:

- **BOUTOUDJ Taous**
- **BENAZIZ Meriem**

Supervisor:

Dr. DAAMOUCHE, IGEE

Miss. WASSILA DIB, CDTA

Registration Number:……/2016

Dedication

I would like to dedicate this modest work to all my family especially my dearest father and mother

To my sisters and their husbands

To my brothers and their wives

To my lovely husband Djamal and all his family

To my beautiful nephews Farah, Thiziri, Anaîs and Liam

To all my friends and colleagues at INELEC

Taous

I would like to dedicate this modest work to all my family especially my mother

To the memory of my father

To my sister Lilya and her husband

To my brothers Samy, Ayoub and Oussama

To my dear husband Khaled and all his family

To my beautiful nephew Ritel

To all my friends and colleagues at INELEC

To my best friends Lina, Lydia, Maya, Massi, Baya and Nada

Meriem

Acknowledgment

Thanks to ALLAH, our final year project is successfully accomplished

*We are highly indebted to our supervisor **Dr. DAAMOUCHE** for his great support and encouragement regarding the fulfillment of this project.*

*We would like to express our gratitude for all the staffs in CDTA, especially to our co-supervisor **Miss WASSILA DIB** and her colleague **OUSSAMA KERDJIDJ** for their kind co-operation, encouragement and guidance what was the main reason for accomplishing successfully our work.*

Our gratitude goes also to Dr. FERHAT from CHU Mustapha, without his help, we could not finalize our database

Our thanks and appreciations also go to all the people and our colleagues in the institute who contributed in some way to the work described in this thesis.

Abstract

The detection of QRS complexes is of great importance for the analysis of the electrocardiogram (ECG) signal, which traces the activity of the heart.

ECG signal is the most used non invasive method to acquire the electrical heart activity. Because of its ease of measurement and its availability, the ECG signal is widely used to identify different types of arrhythmias.

In our project, we have used MATLAB to implement two softwares that detect QRS complex by means of both types of digital filters (IIR and FIR). To test the performance of these two implementations, we have used the benchmark MIT-BIH dataset and also we have generated a data base by recording the ECG of different persons at rest and in activity situations, what was done at CDTA by the help of two doctors. Also, the R peak count was done by a doctor from MUSTAPHA Hospital to be able to evaluate our results.

Table of Content

Acknowledgment I
Dedication II
Table of contents III
List of figures V
List of tables VII
List of acronyms VIII
Abstract X
General introduction 01
Chapter 1: Electrocardiogram generalities
Introduction 02
1.1 Anatomy and function of the human heart 02
1.2 The conduction system of the heart 03
1.3 Basics of ECG 04
1.3.1 Importance of ECG 04
1.3.2 Problems identified by ECG 04
1.3.3 ECG recording 05
1.3.3.1 ECG derivations/Leads 05
1.3.3.2 ECG waveform description 07
1.3.3.3 ECG preprocessing 09
1.4 The main properties of ECG 09
1.4.1 Noise present in ECG signal 09
Conclusion 10

Chapter 2: Filtering Generalities
Introduction 11
2.1 ECG Preprocessing 11
2.2 Filters Generalities 11
2.2.1 Definition of discrete time filters 12
2.2.2 Types of discrete time filters 12
2.2.3 Digital Filters 13

2.3 IIR and FIR filters 14
2.3.1 Finite Impulse Response (FIR) filters 14
2.3.1.1 Basic network for FIR filters 15
2.3.1.2 Frequency response 15
2.3.1.3 Transfer function 16
2.3.1.4 FIR Filter design 16
2.3.1.5 FIR Filter Implementation 16
2.3.2 Infinite Impulse Response (IIR) filter 18
2.3.2.1 Design and Implementation 18
2.3.2.2 Transfer function derivation 19
2.3.2.3 Stability 20

Table of Content

2.3.2.4 Design of IIR filter……20
2.3.2.5 Common filters…..…….22

Conclusion……..…….23

Chapter 3: QSR detection algorithms
Introduction ……..…24
3.1 Pan & Tompkins Algorithm……...24
3.1.1 Band Pass Filtering ……..25
3.1.2 Derivative Operator……..25
3.1.3 Squaring……....26
3.1.4 Integration……..…27
3.2 FFT algorithm……26
3.3 Wavelet algorithm……..27
Conclusion……30

Chapter 4: Simulation reports
Introduction……..…31
4.1 Hardware description…….....31
4.1.1 Electrodes and patches……..31
4.1.2 Shimmer device……31
4.1.2.1 Pairing a Shimmer……32
4.1.2.2 Setting up a shimmer data stream……..32
4.1.2.3 Connect to a shimmer……32
4.1.2.4 Stream from the shimmer……..32
4.1.3 Case used ECG data base…….....33
4.1.3.1 MIT-BIH arrhythmia database……..33
4.1.3.2 Recorded database……33
4.1.4 Simulation and results…….…..34
4.1.4.1 Results of simulation of Pan&Tompkins program using……..34
MIT-BIH database
4.1.4.2 Results of simulation of FFT program using……35
MIT-BIH database
4.1.4.3 MIT-BIH simulation results discussion……38
4.1.4.4 Results of simulation of Pan&Tompkins program using……..38
our recorded database
4.1.4.5 Results of simulation of FFT program using……40
recoded database.
4.1.5 Results discussion……41

Conclusion……42
General conclusion……43
References……IX

General introduction

The primary function of the heart is to pump oxygen-rich blood throughout the body. The heart is composed of muscle cells, which produces the contractions; these cells form the conduction system that allows to an electrical impulse to spread throughout the heart. A cardiac cycle is created when an impulse propagates through the conduction system starting in the atria and going down throw the ventricles, so the impulse is triggered in the atria and it precedes the heart contraction. [1]

An electrocardiogram, also called ECG or EKG, is a vital tool that describes the electrical activity of the heart. Every heart contraction produces an electrical impulse detected by electrodes placed on the skin. The heartbeat produces a series of waves with a time variant morphology. These waves are caused by voltage variations of the cardiac cells. Digital signal processing techniques are used to extract useful information from the input signals received from the body.

ECG recordings provide important information about the heart state. Each heartbeat is produced after: atrial depolarization (P wave), ventricular depolarization (QRS) and ventricular repolarization (T wave). These three stages are continuously repeated. Knowing the waves that form the heartbeat is necessary to analyze the ECG signal.

The QRS complex is one of the most important part in the ECG signal, but its detection is difficult since the signal varies along the time and also because of the different types of noise present in it. Since 1980, software QRS detection has been a research topic. Whereas in the early years the performances of the algorithms were determined by its computational load and complexity, nowadays the detection performance is the major objective.

Perfect QRS detection is a first step for heart rate variability analysis. Many approaches exist; first derivative based methods are often used in real time analysis or for large datasets since they do not require computations [2].

One of the most popular single lead first derivative based QRS detection algorithms is that proposed by Pan& Tompkins in 1985, it has been found to have a good accuracy for various beat morphologies. In addition to the above algorithm, we are going to analyze two others: one based on FFT and another based on discrete wavelet transform.

In this work, we aim to design a software system that can detect QRS complexes by means of both types of digital filters Infinite Impulse Response and Finite Impulse Response based on the analysis done by the previously mentioned algorithms.

Chapter 1:

Electrocardiogram Generalities

Chapter2:

Filtering Generalities

Chapter 3:

QSR detection algorithms

Chapter 4:

Simulation reports

Introduction

The study of the function of the human heart may help us to understand how this muscle does regularly and continuously work to pump blood to the body. The heart has an electrical activity that can be represented graphically over time by an electrodiogram (ECG). This record is taken using a certain number of electrodes placed in a specific way on the human skin. The ECG magnitude is only few mV, so this signal is often distorted by different types of noise that can be treated using adequate filters.

1.1 Anatomy and function of the human heart

The heart (Figure1.1) is an organ that pumps oxygenated blood throughout the body and deoxygenated blood to lungs. It is composed of two separate pumps: left pump pumps the blood to peripheral organs, and right pump pumps the blood to lungs. Each pump is composed of two chambers: an atrium and a ventricle [3].

To control the blood flow there exist four valves:

- **The mitral valve**: separates left atrium and ventricle.
- **The tricuspid valve:** separates right atrium and ventricles.
- **Pulmonary valve:** controls the blood flow from heart to lungs.
- **The aortic valve:** directs blood to the body circulation system.

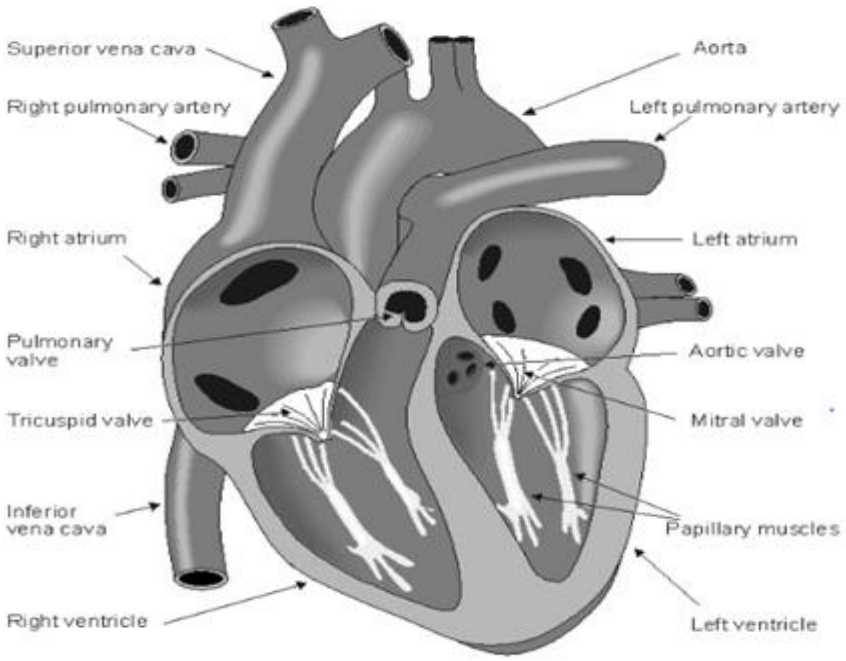

Figure 1.1 : Basic heart anatomy schema- there are four chambers, two on the left (right heart) side responsible for pumping the blood to lungs and two on the right (left heart) responsible for pumping the blood to body [4].

Walls of the heart are formed by cardiac muscle (myocardium) that is responsible on pumping the blood. Specialized muscle cells that conduct electrical impulses control the pumping process. These impulses are called action potential and they are responsible for forming the ECG waveform on the body surface.

Human heart works in periodic cycles to distribute oxygen to whole body. A cycle works as follows:" Deoxygenated blood flows through superior vena cava to the right atrium. When the atrium is contracted, blood is pumped to the right ventricle. From the right ventricle the blood flows through pulmonary artery to the lungs. Lungs remove carbon dioxide from blood cells and replace it with oxygen. Now, the blood is oxygenated; it returns to the left atrium and after another contraction it is pumped to the left ventricle. Finally, the blood is forced out of the heart through aorta to the systemic circulation. The contraction period is called systole, during which the heart fills with blood. The relaxation period is called diastole. From electrical point of view, the cycle has two stages: depolarization (activation) and repolarization (recovery).

1.2 The conduction system of the heart

To maintain the cardiac cycle, the heart developed a special cell system to generate electrical impulses that ensure blood pumping. This system is called conduction system (Figure 1.2). It conveys impulses rapidly through the heart. A cardiac cycle is created when an impulse propagates through the conduction system. The cardiac cycle starts in the atria and goes down throw the ventricles, so the impulse is triggered in the atria and it precedes the heart contraction. [1]

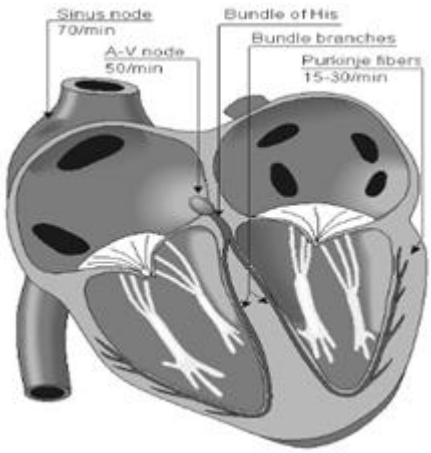

Figure 1.2: Conduction system of the heart consists of Sinus node, Atrioventricular node, Bundle of His, bundle branches and Purkinje fibers [4].

Each cardiac cycle is composed of two stages, contraction (depolarization) and relaxation (repolarization). Depolarization produces a rapid change in the cell potential (from -90 to 20 mV) which causes the depolarization of neighbor cells. After depolarization, these cells come back to their resting stage, produced by the repolarization.

The primary pacemaker of the heart is the sinusoidal node. However, other specialized cells in the heart (AV node, etc.) can also generate impulses but with lower frequency. If the connection from the atria to the atrioventricular node is broken, the AV node is considered as the main pacemaker. If the conduction system fails at the bundle of His, the ventricles will beat at the rate determined by their own region. All cardiac cell types have also different waveform of their action potentials. This is shown in Figure1.3 below:

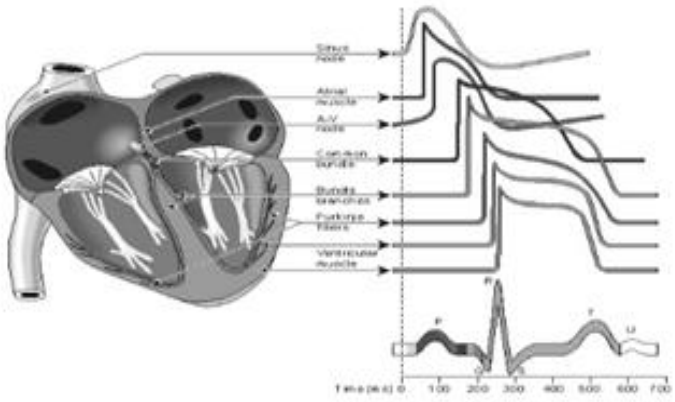

Figure 1.3 Schematic representation of ECG waveform generation by summing of different action potentials [4]

1.3 Basics of ECG

The ECG which is characterized by five peaks and valleys: P, Q, R, S and T displays as a series of electrical waves which represent the electrical activity of the heart. The ECG signal has frequency range of 0.05–100 Hz and its dynamic range is 1–10 mV [5].

1.3.1 Importance of ECG

- It can be used to determine the speed of heart beat.
- Any abnormality in the rhythm of heart beat such as steadiness, disturbances or irregularities can be detected.
- The strength and timing of electrical signals can be detected as they pass through each part of the heart.

1.3.2 Problems identified by ECG

- It is used to detect various cardiac disorders including heart attack and congestive heart failure of a person.
- It can be used to identify diseases such as an enlarged heart that is working under strain, fast, slow or irregular heartbeats called arrhythmias and ventricular tachycardia.

1.3.3 ECG recording

Human body is a good conductor; hence, surface electrodes can be used to measure the heart electrical activity. The projection of summary resultant vector (electrocardiogram) is recorded by electrodes. Different placement of those electrodes provides spatiotemporal variations of the cardiac electrical field. "The difference between a pair of electrodes is referred to as a lead. A large amount of possible lead systems has been invented; depending on a diagnostic purpose, a lead system is chosen and electrodes placed on accurate position. The most commonly used system is the standard 12-lead ECG system defined by Einthoven [6].

I.3.3.1 ECG derivations/Leads

ECG derivations (leads) are the potential difference between two specific points on the human body where measurements are being performed. In general, electrocardiography hardware can measure simultaneously several ECG leads. Each derivation corresponds to a heart contraction in order to capture specific cardio electric field. There exist three types of derivations: limb leads (I, II, III), augmented limb leads (aVI, aVR, aVF), and precordial leads (V1, V2, V3, V4, V5, V6) [7].

- Limb leads

These leads measure potential difference between two points on the human body with respect to the ground potential (bipolar). "Three electrodes are placed triangularly in order to form what's known as Einthoven Triangle" as shown in Figure 1.4 below: [7].

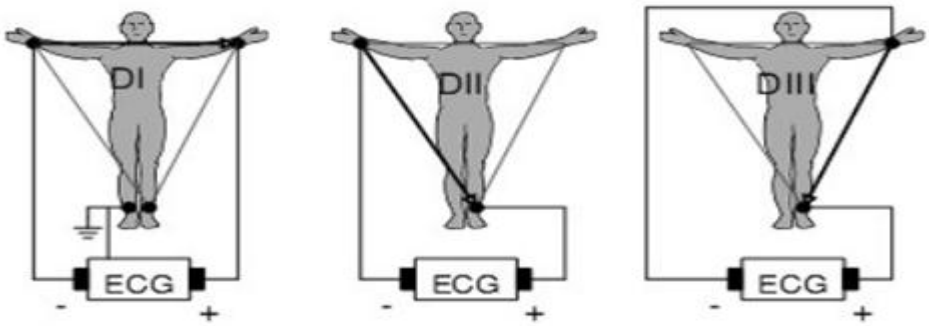

Figure 1.4 : Einthoven triangle electrodes placements for limb derivation [7].

DI (Derivation I): DI = VL−VR

DII (Derivation II): DII = VF – VR

DIII (Derivation III): DIII = VF – VL

Where:VL is the Left Arm Potential, VR, the Right Arm potential, VF, the Left Leg potential.

- **Augmented Leads**

Augmented leads were measured the first time by Wilson who placed the electrodes on the central terminal of Einthoven's triangle (unipolar) derivations (VL, VR, and VF) (Figure1.5). Later on, Augmented leads (aVL, aVR, and aVF) introduced by Goldberger are extracted from the ordinary bipolar leads with an amplification factor of 1.5" [7].

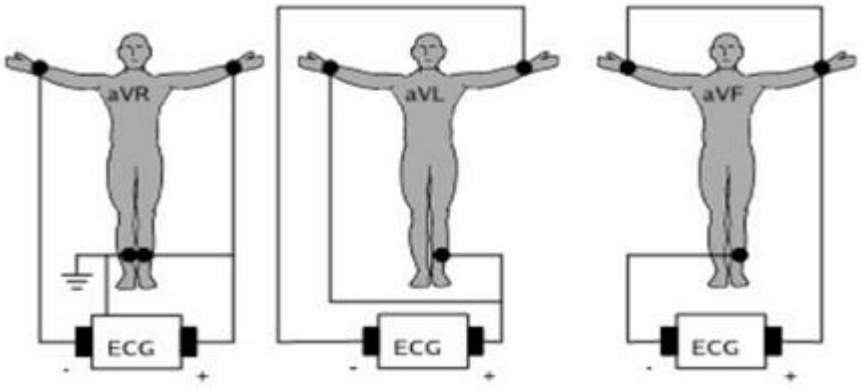

Figure 1.5: Goldberger electrodes placements for augmented limb leads [7].

The electrodes positions are the same as in case of leads I, II and III, but Leads are calculated as the difference between potential of one edge of the triangle and the average of remaining two electrodes (Figure 1.6)

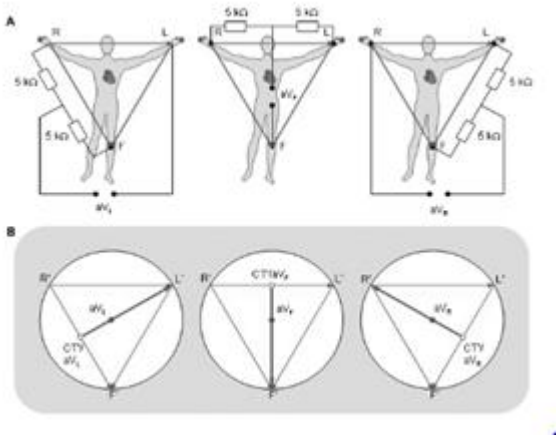

Figure 1.6: Schematic representation of augmented limb leads calculation [4].

- **Precordial leads**

"Unipolar precordinal leads (V1-6 leads) are defined as the difference between potential of electrode on chest and central Wilson terminal. It is constant during cardiac cycle and computed as average of limb leads.Details in Figure1.7.

Precordial leads lie on the horizontal plane, in perpendicular matter to the other leads.

Six electrodes act as the positive poles while Wilson central terminal is used as the negative pole in order to result the six precordial leads".

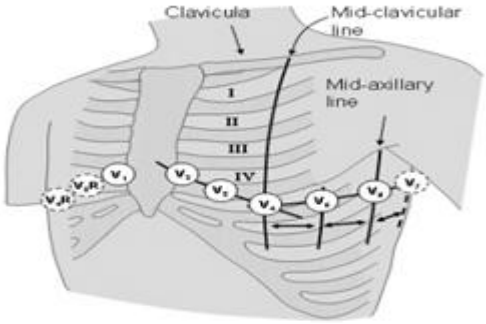

Figure 1.7 : Precordial leads electrodes positions [4].

1.3.3.2 ECG waveform description

A normal ECG signal contains waves, intervals, segments, and one complex defined below:

- **Wave (**P, Q, R, S, T, and U)**:** A positive or negative deflection from baseline
- **Interval (**PR, QT)**:** The time between two specific ECG events.
- **Segment** (ST, TP).**:** the length between two specific points on the ECG signal which are supposed to be at the baseline amplitude.
- **Complex (**QRS)**:** the combination of multiple waves grouped together.

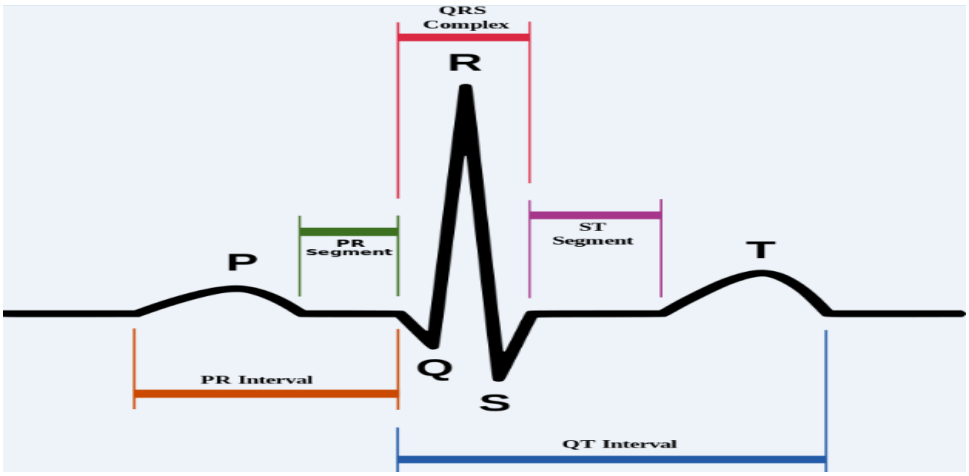

Figure1. 8: Normal ECG waveform [10].

ECG wave has also several peaks and "formations", which is useful for its diagnosis. These are as follows [8]:

- P wave: Represents the wave of depolarization that spreads from the sinus atrioventricular node (SA) throughout the atria, and is usually 0.25mV in amplitude and 80-100 ms length. Each P wave should be followed by a QRS complex.
- PR interval: Reflects the time the electrical impulse takes to travel from the sinus node through the atrioventricular (AV) node and entering the ventricles. It is measured from the beginning of the P wave to the beginning of the QRS complex. The PR interval is usually in the range of 0.12 to 0.2 seconds.
- PR segment: Corresponds to the time between the end of atrial depolarization to the onset of ventricular depolarization. It connects the P wave and the QRS complex; its duration is 50 to 120ms.
- Q wave: Represents the normal left-to-right depolarization of the interventricular septum with an amplitude of about 25% of the R wave [9].
- S wave: Represents late depolarization of the ventricles.
- QRS complex: Is the combination of the Q wave, R wave and S wave. It refelects the rapid depolarization of the right and left ventricles that have a large muscle mass compared to the atria, so the QRS complex usually has much larger amplitude than the P wave. Its duration is 0.08 to 0.12 seconds. The Q and S waves represent negative (downward) deflections on the plot of the lead and the R wave represents positive (upward) deflections.
- S-T segment: the time at which the entire ventricle is depolarized and roughly corresponds to the flat phase of the ventricular action potential. It connects the QRS complex to the T wave with duration of 0.05 to 0.15 seconds.
- Q-T interval: it is measured from the beginning of the QRS complex to the end of the T wave. It represents the time for both ventricular depolarization and repolarization to occur. It ranges from 0.2 to 0.4 seconds depending upon heart rate. (Up to 0.42 seconds in heart rate of 60bpm).
- R wave: Represents early depolarization of the ventricles. A normal value of its amplitude is 1.60mV
- T wave: is a result of ventricular repolarization and is longer in duration than depolarization with an amplitude of 0.1 to 0.5mV.

The main task of the ECG processing is the accurate detection of the QRS complex. This is highlighted by the R peak which is the easiest to detect due to its greatest magnitude. The R peak is a key indicator of heart rate and heart rate variability and can show irregularities such as slow accelerated heart rates. The time interval between the R peaks is known as the R-R intervals. It is used to calculate the heart rate which is calculated by:

$$\frac{Sample\ frequency \times 60}{R_{peak\,2} R_{peak\,1}} = bpm$$

Where: bpm is the heart beats per minute, and $\boldsymbol{R_{peak\,1}}$ **and** $\boldsymbol{R_{peak\,2}}$ are the times of the consecutive peaks.

The normal rate of the heart is from 60 to 100 bpm. So, from the recorded ECG, we can determine whether the heart activity is normal or abnormal.

1.3.3.3 ECG Preprocessing

Heart Rate is inferred by detecting the QRS Complexes and obtaining the period between consecutive R peaks, which is not as simple as it seems because ECG Signals are usually affected by several noise sources, like muscular contraction (EMG) and respiration. Moreover, as a consequence of a disease or a temporal alteration, heart beats can have very different characteristic patterns. Therefore we must suppress this noise for a correct evaluation of ECG.

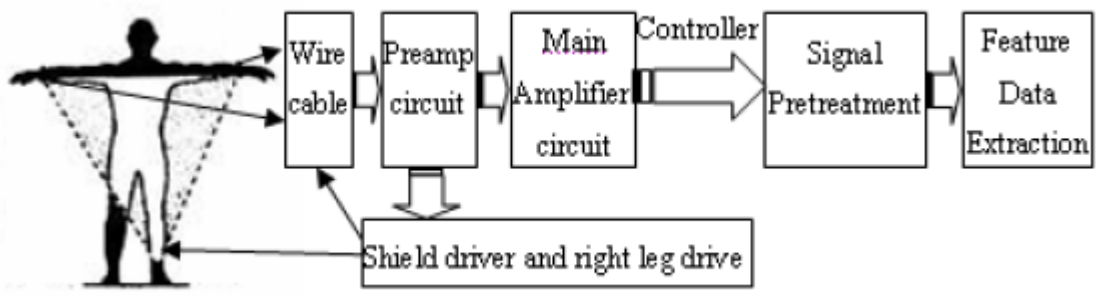

Figure 1.9: ECG signal pretreatment and feature data extraction system chart [11].

1.4 The main properties of ECG

1.4.1 Noise present in ECG signal

Noise sources include:

- **Baseline Drift:** It occurs due to respiration and body movement that can produce a low frequency drift from the desired base line of the signal. It is usually low in frequency, low in amplitude, and of ongoing duration. Typically it is a signal <0.5Hz. This noise can be removed by implementing a high-pass filter with cut-off frequency at nearly 0.5Hz realized in hardware or software [12].

- **Power line interference**: The ECG signal can be affected by power line interference due to the low output levels of the signal. Induction from neighboring equipment or faulty grounding of equipment can lead to ECG leads picking up 50Hz (or 60Hz depending on country) interference from neighboring power line currents. To reduce or remove this unwanted feature, removal of possible interfering equipment and power cables is an effective approach. It is typically fixed frequency, high in amplitude, and of ongoing duration. The amplitude of power-line noise is very large and generally gets coupled into the system, despite care to prevent common-mode noise in the digital domain. Power-line noise is removed by implementing a notch filter at 50/60Hz in the digital domain [13].
- **Electromyography (EMG) noise:** EMG interference is the unwanted electrical activity of muscles not related to the movement of the heart that can interfere with the EMG. It is typically high in frequency (broadband (20-1000Hz)), low in amplitude (10% ECG), and of variable duration This type of noise can be lessened by reducing movement of the patient..or the use of a low pass filter with cut-off frequency >40 Hz.
- **Flat line/ missing lead:** Due to a bad electrode-to-skin contact or electrodes' disconnection.
- **Low amplitude signal:** A persistent low amplitude signal in some leads may be produced by an increased electrode-to-skin impedance. It might appear as sudden changes from normal to low amplitudes and vice-versa.
- **Steep slope/Spike noise:** high frequency noise caused by abrupt movement of the electrodes can produce distorted QRS, known erroneous/spurious beats [14].

Adequate filtering techniques need to be utilized to limit the effect of the discussed noise sources to ensure accurate signal processing. The characterization of the noise sources should provide a basis for proper filter design. Many studies have already been performed to evaluate the effectiveness of various filtering techniques for ECG signals [15], [16] because the choice of the filter will greatly influence the performance of the processing algorithms so it should be chosen very carefully.

Conclusion

The heart is a very organized organ, it has some electrical activity that can be measured by electrodes placed on the skin; some standardized systems has been developed for the electrode placement in the recording of ECG where even this placement may cause one type of different types of noise that must be removed using both FIR and IIR filters

Chapter 2 Filtering generalities

Introduction

In this chapter we are going to introduce theoretical background concerned with signal processing and filter design techniques widely used for ECG preprocessing. We mainly focused on the two commonly used filters: Finite Impulse Response (FIR) and Infinite Impulse Response (IIR).

2.1 ECG preprocessing

ECG preprocessing is treating the ECG signal before extracting its useful information. Different methods are used in the design of the filters used to remove unwanted parts of the signal or the different types of noise present such as the power line interference which is the most common ECG noise. We need first to determine the type of noise then the corresponding filter design and implementation to cancel it. Filtering is also used to isolate desired parts of the signal, such as the components lying within a certain frequency range. [17]

Linear phase filtering is mainly used to prevent phase distortion from altering various wave properties of the cardiac cycle such as the duration of the QRS complex, the ST–T, or the endpoint of the T wave. FIR filters can have a linear phase response, provided that the impulse response is either symmetric or anti-symmetric; however, FIR designs result in high filter orders.

2.2 Filters generalities

Filters, whether analog or digital, remove selected frequencies and are named according to their range of allowed frequencies(lowpass, highpass, bandpass, bandstop). Any filter is characterized by its type, order, bandwidth.

- Analog Filter: uses analog electronic circuits made up from components such as resistors, capacitors and operational amplifiers to produce the required filtering result. The input may be electrical voltage or current to get then a filtered output.
- Digital Filter: uses a digital processor to perform numerical calculations on sampled values of the signal. The processor may be a general purpose computer such as a PC, or a specialized DSP chip. The analog input signal is first sampled and digitized using analog to digital converter (ADC). The result, representing successive sampled values of the signal, is transferred to the processor to carry out numerical calculations on them, then; the results representing sampled values of the filtered signal are output through a digital to analog converter (DAC) converting back the signal to analog form.

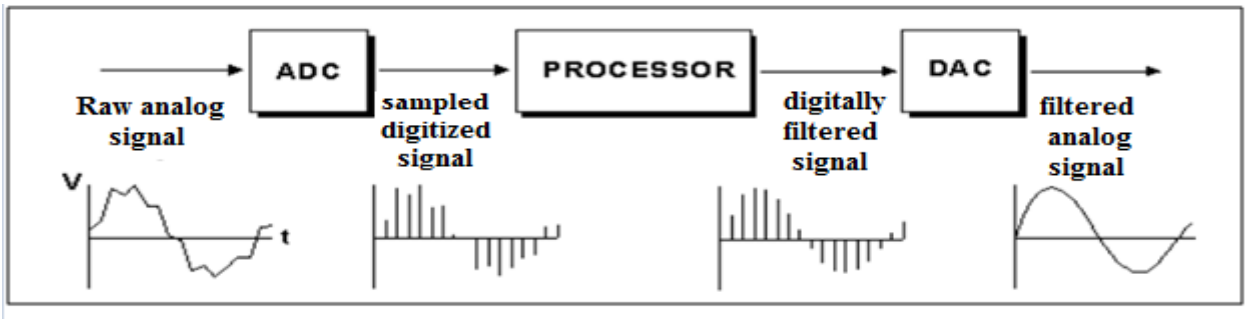

Figure 2.1: Digital Filter Stages

2.2.1 Definition of discrete time filters

A discrete time filter is a discrete time linear time invariant system characterized by its frequency response or a difference equation (constant coefficients DE).

2.2.2 Types of discrete time filters

- Low-pass filters: Allow a low frequency band of a signal to pass through and attenuate a high frequency band.
- Band-pass filters: Allow intermediate frequency bands of a signal to pass through and attenuate both low and high frequency bands.
- High-pass filters: Allow a high frequency band of a signal to pass through and attenuate a low frequency band.
- Band reject filters: Allow both low and high frequency bands of a signal to pass through and attenuate intermediate frequency bands.

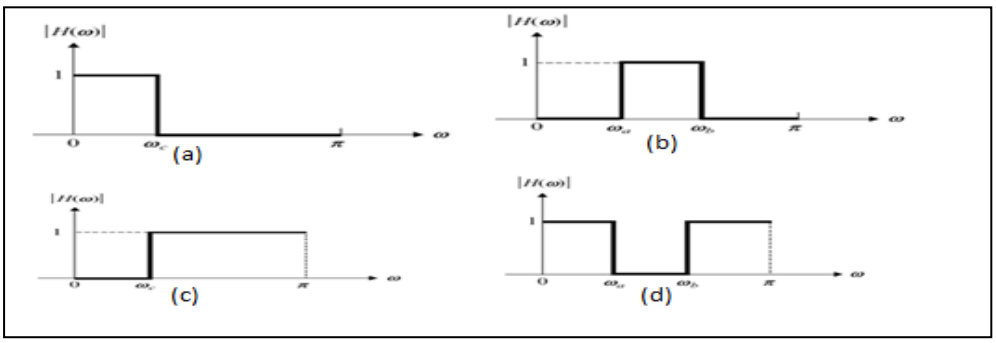

Figure 2.2: (a): Low-Pass Filter, (B) Band-Pass Filter, (C) High-Pass Filter (D) Band Reject Filter

- Allpass filters: Allow all frequency components to pass through.
- Finite impulse response (FIR) filters: They are bounded input bounded output stable and the impulse response has finite time and it uses a finite number of samples. It is a filter structure with a finite number of samples that can be used to implement almost any sort of frequency response digitally. It is usually implemented using a series of delays, multipliers, and adders to create the output.

  Figure2.3 shows the basic block diagram for an FIR filter of order N. the h_k values are the coefficients used for multiplication, so that the output at time n is the summation of all the delayed samples multiplied by the appropriate coefficients.

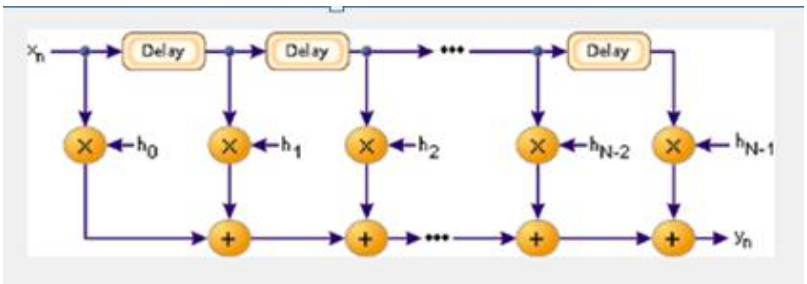

Figure 2.3: The Logical Structure of an FIR Filter

- Infinite impulse response (IIR) filters: The impulse response has infinite time. It is also called recursive filter because the output depends on past inputs and past outputs. Its design is not guaranteed to be stable since it has zeros and poles.

2.2.3 Digital Filters

Filters are used in ECG preprocessing for eliminating all types of ECG contaminations of noise and artifacts, and smoothing it. There are two types of digital filters: Infinite Impulse Response (IIR) and Finite Impulse Response (FIR). Figure2.4 shows a realistic versus ideal filter response.

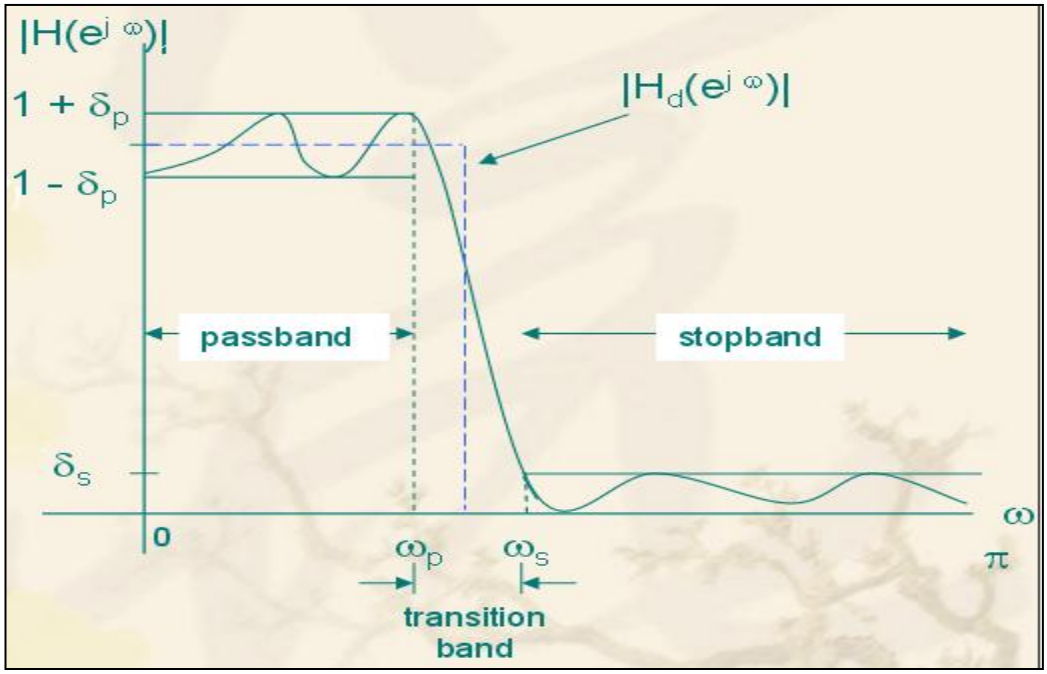

Figure2.4: Realistic versus Ideal Filter Response[18**]**

- Notations:
  - ✓ $|H(e^{jw})|$: Magnitude response of a filter.
  - ✓ $|H_d(e^{jw})|$: The desired magnitude response of the filter.
  - ✓ δ_b andδ_s :maximum passband and stopband ripple magnitudes.
  - ✓ ω_p and ω_s:passband and stopband frequencies, respectively.
  - ✓ N: filter order.

2.3 IIR and FIR filters

There are two primary types of digital filters used in DSP applications: Finite Impulse Response (FIR) and Infinite Impulse Response (IIR). As shown in Figure 2.5.

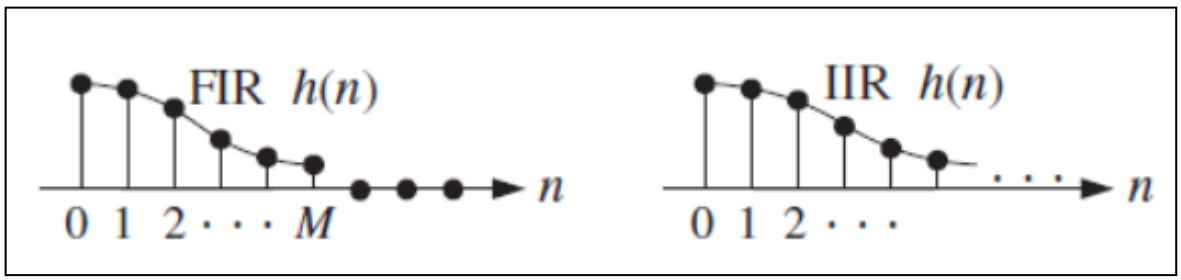

Figure 2.5: Impulse responses of FIR and IIR filters.

The transfer function of the filter is:

$$H(z) = \frac{Y(z)}{X(z)} = \frac{\sum_{k=0}^{M} b_k z^{-k}}{1 + \sum_{k=1}^{N} a_k z^{-k}} \qquad (2.1)$$

2.3.1 Finite Impulse Response (FIR) filters

FIR filter is a filter whose response to any finite length input is of finite duration, hence it settles to zero in finite time. The impulse response of an N^{th}order FIR filter has $N + 1$ nonzero samples on finite time interval [0, N]. FIR filters can be discrete or continuous time, and digital or analog [19].

$$\{h[0], h[1], h[2], \ldots, h[N]\}$$

Where: $N = L - 1$ is the order of the filter and L is the length of the filter.

FIR filters do not use feedback. For an FIR filter with L coefficients, the output always becomes zero after a given t.

FIR filters have a number of useful properties:

- Require no feedback. This means that any rounding errors are not accumulated by summed iterations. This also makes implementation simpler.
- Do not contain poles, they just have zeros, hence they are inherently stable, since the output is a sum of a finite number of finite multiples of the input values.
- Can easily be designed to be linear phase by making the coefficient sequence symmetric.

The main disadvantage of FIR filters is that it requires more computation compared to an IIR filter.

2.3.1.1 Basic network for FIR filters

$$y[n] = \sum_{k=0}^{N} b_k x(n-k) = \sum_{k=0}^{N} h[k]x[n-k] \quad (2.2)$$

or: $$y[n] = h[0]x[n] + h[1]x[n-1] + \cdots + h[N]x[n-N] \quad (2.3)$$

Where:

- $x[n]$:The input signal.
- $y[n]$: The output signal.
- N: is the filter order.
- $h[i]$: Is the i^{th}value of the impulse response for $0 \leq i \leq N$

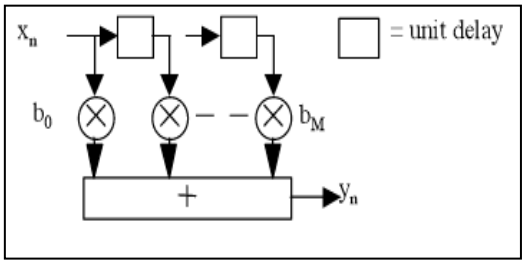

Figure2.6: A structure of an FIR filter

The impulse response is nonzero over a finite length $N+1$, and can be obtained, with $x[n] = \delta[n]$ and including zeros as follows:

$$\mathrm{h[n]} = \mathrm{y[n]} = \sum_{\mathrm{k=0}}^{\mathrm{M-1}} \mathrm{b_k}.\,\delta[\mathrm{n-k}] = \begin{cases} \mathrm{b_n} & 0 \leq \mathrm{n} \leq \mathrm{N} \\ 0 & \text{otherwise.} \end{cases} \quad (2.4)$$

2.3.1.2 Frequency response

The effect of the filter on the sequence $x[n]$ is described in the frequency domain by the convolution theorem:

$$\underbrace{\boldsymbol{F\{x * h\}}}_{\boldsymbol{Y(w)}} = \underbrace{\boldsymbol{F\{x\}}}_{\boldsymbol{X(w)}}.\underbrace{\boldsymbol{F\{h\}}}_{\boldsymbol{H(w)}} \text{ and } \boldsymbol{y[n] = x[n] * h[n] = F^{-1}\{X(w).H(w)\}} \quad (2.5)$$

Where F and F^{-1} denote the discrete time Fourier transform (DTFT) and its inverse, respectively. Therefore, the complex valued, multiplicative function $H(w)$ is the frequency response of the filter. It is defined by:

$$H_{2\pi}(w) = \sum_{n=-\infty}^{\infty} h[n].(e^{iw})^{-n} = \sum_{n=0}^{N} b_n.(e^{iw})^{-n} \quad (2.6)$$

Where, the added subscript denotes 2π periodicity, w represents frequency in normalized units (radians/sample). The substitution $w = 2\pi f$ changes the units of frequency (f) to cycles/samples and the periodicity to 1. When the $x[n]$ sequence has a known sampling rate, f_s samples/second, the substitution $w = 2\pi f/f_s$ changes the units of frequency (f) to cycles/second (hertz) and the periodicity to f_s. The value $w = \pi$ corresponds to a frequency of $f = \frac{f_s}{2} Hz = \frac{1}{2} cycles/samples,$ which is the Nyquist frequency.

2.3.1.3 Transfer function

The transfer function of an FIR filter has only a numerator. All of the coefficients (feedback terms) are zero and the filter has no finite poles.

The frequency response,$H_{2\pi}(w)$, can also be written as $H(e^{jw})$, where function $H(z)$ is the Z transform of the impulse response:

$$H(z) = \sum_{n=-\infty}^{\infty} h[n].z^{-n} \tag{2.7}$$

One cycle of the periodic frequency response can be found in the region defined by $z = e^{jw}$, $-\pi \leq \omega \leq \pi$, which is the unit circle of the Z- plane.

2.3.1.4 FIR Filter Design

An FIR filter is designed by finding the coefficients and filter order that meet certain specifications, which can be in the time domain or the frequency domain.

2.3.1.5 FIR Filter Implementation

FIR filters have only zeros (no poles). They are also known as all zero filters, feedforward or non-recursive, or transversal filters. There exist four types of linear phase FIR filters:

- **Linear phase FIR filters**

An FIR is called linear phase if it satisfies: $h[n] = \pm h[N-n]$

✓ **Type 1**: most versatile. The order is even: $N = 2M$ and $h[n] = h[N-n]$

$$H\left(e^{jw}\right) = \sum_{n=0}^{2M} h[n] \tag{2.8}$$

Then:

$$H\left(e^{jw}\right) = e^{-jwn}\left\{\sum_{n=0}^{M-1} h[n]\, e^{jw(M-n)} + h[M] + \sum_{n=M+1}^{2M} h[n]\, e^{jw(M-n)}\right\} \tag{2.9}$$

So:

$$H\left(e^{jw}\right) = e^{-jwn}\left\{h[M] + \sum_{n=0}^{M-1} 2\, h[n] \cos[w(M-n)]\right\} \tag{2.10}$$

✓ **Type 2**: Symmetric impulse response: $h[n] = h[N-n]$, and the order is odd: $N = 2M+1$.

$$H(e^{jw}) = \sum_{n=0}^{2M+1} h[n]\, e^{-jwn} \tag{2.11}$$

$$H(e^{jw}) = e^{-jw\left(M+\frac{1}{2}\right)}\left\{\sum_{n=0}^{M} h[n]\, e^{jw\left(M+\frac{1}{2}-n\right)} + \sum_{n=M+1}^{2M+1} h[n] e^{jw\left(M+\frac{1}{2}-n\right)}\right\} \tag{2.12}$$

Rearranging:

$$H(e^{jw}) = e^{-jw(M+\frac{1}{2})}.2\sum_{n=0}^{M} h[n]\cos\left[w\left(M+\frac{1}{2}-n\right)\right] \tag{2.13}$$

The amplitude response is real and is given by:

$$A_{II}(w) = 2\sum_{n=0}^{M} h[n]\cos\left[w\left(M+\frac{1}{2}-n\right)\right] \tag{2.14}$$

Then at $w = \pi$, we get: $A_{II}(\pi) = 0$

The frequency response is always 0 at $= \pi$, therefore type 2 filters are not suitable for designing high pass filters and band-reject filters.

✓ **Type 3**: anti-symmetric impulse response: $h[n] = -h[N-n]$, and$N = 2M$ (N even):

$$H(e^{jw}) = e^{-jwM}\left\{\sum_{n=0}^{M-1} h[n]\, e^{jw(M-n)} + \sum_{n=M+1}^{M} h[n] e^{jw(M-n)}\right\} \tag{2.15}$$

Then:

$$H(e^{jw}) = e^{-jwM} e^{j\frac{\pi}{2}} \sum_{n=0}^{M-1} 2h[n]\sin[w(M-n)] \tag{2.16}$$

The response is purely imaginary and its amplitude is given by:

$$A_{III}(w) = \sum_{n=0}^{M-1} 2h[n]\sin[w(M-n)] \tag{2.17}$$

It is obvious that $A_{III}(0) = A_{III}(\pi) = 0$

Therefore, type III filters are not suitable for high pass, low pass and band reject filters. It is suitable only for band pass filters; sometimes it is used for Hilbert transform and differentiators.

✓**Type 4**: The impulse response is anti-symmetric:$h[n] = -h[N-n]$, and the order is odd: N=2M+1.

$$H(e^{jw}) = e^{-jw(M+\frac{1}{2})}\left\{\sum_{n=0}^{M} h[n]\, e^{jw\left(M+\frac{1}{2}-n\right)} + \sum_{n=0}^{M} h[N-n]e^{-jw\left(M+\frac{1}{2}-n\right)}\right\} \quad (2.18)$$

Then:

$$H(e^{jw}) = e^{-jw\left(M+\frac{1}{2}\right)}\left\{2j\sum_{n=0}^{M} h[n]\sin\left[w\left(M+\frac{1}{2}-n\right)\right]\right\} \quad (2.19)$$

The amplitude response is:

$$A_{IV}(w) = 2\sum_{n=0}^{M} h[n]\sin\left[w\left(M+\frac{1}{2}-n\right)\right] \quad (2.20)$$

At $w = 0$, we get:$A_{IV}(w) = 0$. Type IV filters are not suitable neither as a low pass filters nor as band stop filters.

2.3.2 Infinite Impulse Response (IIR) filters

Infinite impulse response filters have an infinite impulse response$h(t)$thatdoes not become exactly zero for $t > T$ with some finite T, but continue indefinitely [19].

The impulse response is infinite because there is feedback in the filter.

A property of an IIR filter compared to an FIR filter is its efficiency in implementation since it can achieve a given filtering characteristic using less memory and calculations accomplished with lower order. However as a direct consequent of feedback, when the output is not computed perfectly and is fed back, the error will compound.

2.3.2.1 Design and Implementation

IIR response is created with the presence of feedback as shown in the block diagram. The z domain transfer function of an IIR filter describes these feedback terms by a non-trivial denominator or poles [19]. Figure2.8 shows a block diagram of an IIR filter. With the z^{-1}represents a unit delay.

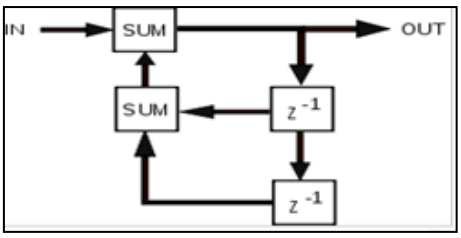

Figure 2.7: Block diagram of an IIR filter

2.3.2.2 Transfer function derivation

The transfer function of IIR analog filters is converted to z domain using certain mathematical techniques such as the bilinear transform, impulse invariance. Digital IIR filters design is usually based on analog filters such as the Chebyshev filter, Butterworth filter, and Elliptic filter.

Digital filters are mainly described and implemented in terms of the difference equation that defines how the output signal is related to the input signal:

$$y[n] = \frac{1}{a_0}\left(b_0 x[n] + b_1 x[n-1] + \cdots + b_p x[n-p] - a_1 y[n-1] - a_2 y[n-2] - \cdots - a_Q y[n-Q]\right) \quad (2.21)$$

Where:

- p is the feedforward filter order.
- b_i are the feedforward filter coefficients.
- Q is the feedback filter order.
- a_i are the feedback filter coefficients.
- $x[n]$ is the input signal.
- $y[n]$ is the output signal.

This can be written as:

$$y[n] = \frac{1}{a_0}\left(\sum_{i=0}^{p} b_i x[n-1] - \sum_{j=1}^{Q} a_j y[n-j]\right) \quad (2.22)$$

Which , when rearranged, becomes:

$$\sum_{j=0}^{Q} a_j y[n-j] = \sum_{i=0}^{p} b_i x[n-i] \quad (2.23)$$

To find the transfer function of the filter, we first take the Z-transform of each side of the above equation, where we use the time shift property to obtain:

$$\sum_{j=0}^{Q} a_j z^{-j} Y(z) = \sum_{i=0}^{p} b_i z^{-i} X(z) \quad (2.24)$$

The obtained transfer function is defined to be:

$$H(z) = \frac{Y(z)}{X(z)} = \frac{\sum_{i=0}^{p} b_i z^{-i}}{\sum_{j=0}^{Q} a_j z^{-j}} \quad (2.25)$$

Considering that in most IIR filter designs coefficient a_0 is 1, the IIR filter transfer functionwill be:

$$H(z) = \frac{\sum_{i=0}^{p} b_i z^{-i}}{1 + \sum_{j=1}^{Q} a_j z^{-j}} \quad (2.26)$$

2.3.2.3 Stability

The BIBO stability criterion requires that the region of convergence (ROC) of the system includes the unit circle in the z plane.

The poles are defined as the values of Zwhich make the denominator of $H(z)$equal to 0:

$$0 = \sum_{j=0}^{Q} a_j z^{-j} \quad (2.27)$$

Clearly, if $a_j \neq 0$, the poles are not located at the origin of the z plane as they are for FIR filters.

IIR filters are sometimes preferred over FIR filters because an IIR filter can achieve a much sharper transition region roll-off than an FIR filter of the same order.

2.3.2.4 Design of IIR filters

There are mainly three types of analog filters:

- Butterworth.
- Chybechev (1,2)
- Elliptic filters

The design of IIR filters starts by the determination of its order; a mapping technique is used to convert the analog impulse response $h(t)$ into a digital impulse response $h[n]$.

❖ **General requirement of mapping technique**

- ✓ Stable filter in S domain should be mapped into stable filter in Z domain
- ✓ Left half plane LHP should be mapped into inside the unit circle
- ✓ Right half plane RHP should be mapped into inside the unit circle
- ✓ $J\Omega$ should be mapped onto the unit circle.

a) Impulse invariance method

H(s) is the Laplace Transform of the analog impulse response. It is intended to obtain $h(n)$ from $h(t)$.

$Th_c(nT) - - - > h[n]$, Where T: the sampling period.

Assuming that $H(s)$ has K distinct poles:

$$H(S) = \frac{N(S)}{D(S)} or H(S) = \sum_{k=0}^{k} \frac{c_k}{s - s_k} \quad (2.28)$$

We have:

$$h(t) = \sum_{k=0}^{k} c_k e^{skt} \; t \geq 0 \quad (2.32)$$

And:

$$h[n] = h(nT) = \sum_{k=0}^{k} c_k e^{s_k nT} \quad (2.32) \quad (2.29)$$

Using the z transform we obtain:

$$H(Z) = Z\{h[n]\} = \sum_{n=-\infty}^{\infty} h[n] z^{-n} \quad (2.30)$$

$$H(z) = \sum_{k=0}^{\infty} \frac{c_k}{1 - e^{s_k T} Z^{-1}} \quad (2.31)$$

We have:

S_K(S domain) is mapped into $e^{s_k T}$

$\mathrm{Re}(S_K) < 0$ is mapped into $|e^{s_k T}| < 1$: Inside the unit circle.

$\mathrm{Re}(S_K) > 0$ is mapped into $|e^{s_k T}| > 1$: Outside the unit circle.

$\mathrm{Re}(S_K) = 0$ is mapped into $|e^{s_k T}| = 1$: On the unit circle.

The impulse invariance method is suitable only for lowpass signals and not suitable for highpass signals because of aliasing.

b) Bilinear Transformation Method

We have:

$$H(s) = \frac{X(s)}{Y(s)} = \frac{b}{s+a} \rightarrow sY(s) + aY(s) = bX(s) \quad (2.32)$$

Using the inverse Laplace transform:

$$\frac{dy(t)}{dx(t)} + ay(t) = bx(t) \quad (2.33)$$

Integrating yields:

$$y(nT) = \frac{T}{2}[-a\dot{y}(nT - T) + \dot{y}(nT)] + y(nT - T) \quad (2.34)$$

Since: $y(t) = -a\dot{y}(t) + bx(t)$we get:

$$y[n][1 + a\frac{T}{2}] = y[n-1][1 - a\frac{T}{2}] + b\frac{T}{2}(x[n-1] + x[n]) \quad (2.35)$$

Using the z transform:

$$Y(z)(1 - a\frac{T}{2}) = z^{-1}Y(z)(1 - a\frac{T}{2}) + b\frac{T}{2}X(z)(z^{-1} + 1) \quad (2.36)$$

Since: $H(z) = \frac{Y(Z)}{X(Z)}$ then:

$$H(z) = \frac{b}{a + \frac{2}{\mathrm{T}}\frac{1-z^{-1}}{1+z^{-1}}} \quad (2.37)$$

Where:$S = \frac{2}{T}\frac{1-z^{-1}}{1+z^{-1}}$ is the bilinear transformation.

2.3.2.5 Common filters

a) Butterworth filter

It has a smooth response in both the pass band and stop band, its analog frequency response is given by:

$$|H(S)|^2 = \frac{1}{1+(\frac{s}{j\Omega_S})^{2N}} \quad (2.38)$$

The poles are given by: $\mathrm{s} = \mathrm{j}\Omega_c e^{\frac{j\pi}{2}}(-1)^{\frac{1}{2N}}$ or $\mathrm{s} = \Omega_c e^{\frac{j\pi}{2}}(e^{j\pi(2k+1)})^{\frac{1}{2N}}$

Then:

$$s_k = \Omega_c e^{\frac{j\pi(2k+1+N)}{2N}} \qquad 0 \le k \le 2N-1 \quad (2.39)$$

Stability requirement implies that only roots with negative real part are retained, so: $0 \le k \le N-1$

b) Chebyshev filter

ChebychevI has ripples in the pass band and monotonic in the stop band, it contains poles and does not have zeros.

The general formula of type-I Chebyshev filter is given by:

$$|H(\Omega)|^2 = \frac{1}{1 + \xi^2 {T_N}^2(\frac{\Omega}{\Omega_P})} \quad (2.40)$$

The general formula of type-II Chebyshev filter is given by:

$$|H(\Omega)|^2 = \frac{1}{1 + \frac{\xi^2 {T_N}^2(\frac{\Omega_S}{\Omega_P})}{{T_N}^2\frac{\Omega_S}{\Omega}}} \quad (2.41)$$

Where:

- ξ : Parameter that controls the amount of pass band ripple.
- T_N : Is the N^{th} order chebyshev polynomial.
- Ω_s : The stop band frequency.
- Ω_P : The pass band frequency.

Conclusion

This chapter was about filtering concepts. Different filters are used; most of common properties of FIR and IIR filters are highlighted. Also, mostly used windowing methods are detailed.

In addition, two different mapping methods are explained namely impulse invariance and bilinear transformation.

Chapter3: QRS detection algorithms

Introduction

Detection of QRS Complexes in ECG signals is an important step in the study of cardiac characteristics to determine heart rate. ECG Signals are usually affected by noise of low and high frequencies. Several methods have been proposed to filter out the noise and detect the characteristic pattern of QRS complex.

Most of QRS detection algorithms are based on two stages: preprocessing and decision [20]. In the preprocessing stage different techniques are applied to the signal to filter out and smooth the signal in order to attenuate P and T waves as well as the noise. While in the decision stage the most important task is the determination of thresholds.
We are going to introduce three widely used algorithms for QRS detection:

- Pan & Tompkins algorithm
- FFT algorithm
- Wavelet algorithm

3.1 Pan & Tompkins algorithm

It is one of the most important QRS detection algorithms. The R wave slope is the basic feature to locate the QRS complex; however it is insufficient for efficient QRS detection. Hence, this algorithm analysis is based on the slope, amplitude and width of the signal.[21]

The algorithm implements a digital band pass filter which can reduce false detection caused by the various types of interference present in the ECG signal. This filtering permits the use of low thresholds, thereby increases the detection sensitivity [22].

Figure3.1 below shows a graphical representation of the basic steps of this algorithm.

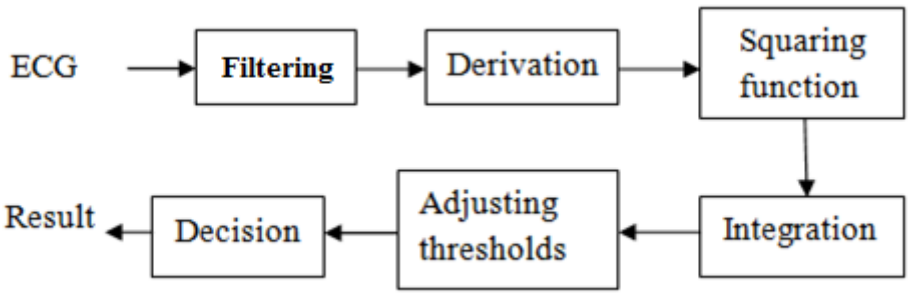

Figure3.1: Block diagram of Pan & Tompkins algorithm.

The signal passes through filtering, derivation, squaring, and integration phases before thresholds are set and QRS complexes are detected [21].

3.1.1 Band pass filtering

The use of the band pass filter for QRS detection reduces noise in the ECG. The band pass filtering maximizes the QRS energy in the 5Hz-40Hz range. The filter implemented in this algorithm is composed of cascaded high pass and low pass Butterworth IIR filters.

In the first step, the algorithm passes the signal through a low-pass and a high-pass filter in order to reduce the effect of the muscle noise, the power line interference, the baseline wander, and the T wave interference.

The transfer function of the second order low pass filter is:

$$H(z) = \frac{(1-z^{-6})^2}{(1-z^{-1})^2} \quad (3.1)$$

The gain is 36 and the filter processing delay is 6 samples.

The low-pass filter is described by the formula:

$$y(n) = 2y(n-1) - y(n-2) + x(n) - 2x(n-6) + x(n-12) \quad (3.2)$$

And the high-pass filter is given by:

$$y(n) = y(n-1) - \frac{1}{32}x(n) + x(n-16) - x(n-17) + \frac{1}{32}x(n-32) \quad (3.3)$$

With the transfer function:

$$H(z) = \frac{(-1 + 32z^{-16} - 32z^{-17} + z^{-32})}{(1-z^{-1})} \quad (3.4)$$

The cutoff frequency of this filter is about 5Hz, the gain is 32, and the delay is 16 samples.

3.1.2 Derivative Operator

The second step after filtering is differentiation. It is done to extract the QRS slope information using the following formula:

$$y(n) = \frac{1}{8}[2x(n) + x(n-1) - x(n-3) - 2x(n-4)] \quad (3.5)$$

The derivation suppresses the low frequency components of P and T waves, and provides a large gain to the high frequency components arising from the high slopes of the QRS complex.

3.1.3 Squaring

The squaring operation makes the result positive and emphasizes large differences resulting from QRS complexes; the small differences arising from P and T waves are suppressed. The high frequency components in the signal related to the QRS complex are further enhanced. It is a nonlinear transformation that consists of point by point squaring of the signal samples making all data point positive and emphasizing the higher frequencies.

$$y(n) = x^2(n) \qquad (3.6)$$

3.1.4 Integration

The following step concerned with passing the squared waveform through a moving window integrator. This integrator sums the area under the squared waveform over a suitable interval, advances one sample interval, and integrates the new predefined interval window. The half width of the window has been chosen as 27 to include the time duration of extended abnormal QRS complexes, but short enough that it does not overlap both a QRS complex and a T wave. Moving Average (MA) filter extracts the slope of the R wave. It is implemented with the following difference equation:

$$y(n) = \frac{1}{N}\left[x\big(n-(N-1)\big) + x\big(n-(N-2)\big) + \cdots + x(n)\right] \qquad (3.7)$$

Where N=1+2M is the number of samples in the width of the moving window. M is half width of moving average filter.

A temporal location of the QRS is marked from the rising edge of the integrated waveform.

In the last step two thresholds are adjusted. The higher of the two thresholds identifies peaks of the signal. The lower threshold is used when no peak has been detected by the higher threshold in a certain time interval. In this case the algorithm searches back for a lost peak. When a new peak is identified as a local maximum change in direction within a predefined time interval then it is classified as a signal peak if it exceeds the high thresholds, or as a noise peak otherwise.

To be identified as a QRS complex, a peak must be recognized as a QRS in both integration and filtered waveform.

3.2 FFT algorithm

Fourier Transform is an algorithm that transforms a signal from time domain into frequency domain, often called the spectrum of the signal.

The fast fourier transform (FFT) is a discrete Fourier tansform algorithm which reduces the number of computations needed for N points from $2N^2$ to $\frac{N}{2}logN$, where log is the base-2 logarithm[19].

FFT algorithms generally fall into two classes: decimation in time, and decimation in frequency.

The basic idea is to break up a transform of length N into two transforms of length $\frac{N}{2}$ using the identity[19]:

$$\sum_{n=0}^{N-1} a_n e^{\frac{-2\pi nk}{N}} = \sum_{n=0}^{\frac{N}{2}} a_{2n} e^{\frac{-2\pi(2n)k}{N}} + \sum_{n=0}^{\frac{N}{2}} a_{2n+1} e^{\frac{-2\pi(2n+1)k}{N}} \qquad (3.8)$$

$$= \sum_{n=0}^{\frac{N}{2}} a_n^{even} e^{\frac{-2\pi nk}{\frac{N}{2}}} + e^{\frac{-2\pi k}{N}} \sum_{n=0}^{\frac{N}{2}-1} a_n^{odd} e^{\frac{-2\pi nk}{\frac{N}{2}}}$$

ECG signals can be processed using Fast Fourier Transform .The total process of FFT method consists of the following steps:

- Read the data base
- Apply a median filter of order 100 to eliminate the DC drift:

The principle here is to apply a median filter f1 (N=100) on the original signal (ecg1). The corrected signal ecg3 is obtained from the subtraction of the filtered signals ecg2 from the original signal ecg1.

ecg2 = ecg1* f1 (3.9)

ecg3 = ecg1– ecg2 (3.10)

- Apply FFT on ecg3 to transform it into frequency domain. Then, remove the lower frequencies, now the obtained signal ecg4 has only high frequencies. The inverse FFT is then applied on ecg4 to get a time domain signal ecg5. After windowing, the peaks R are detected.

3.3 Wavelet algorithm:

A wavelet transform is a mathematical tool that decomposes a signal into a set of waveforms localized both in time and frequency domains. The decomposition produces coefficients, which are functions of the scale of the wavelet function and position which is a shift across the signal [23].

The Discrete Wavelet Transform (DWT) provides sufficient information for analyzing the original signal, with a significant reduction in the computation time.

Filters of different cutoff frequencies are used to analyze the signal at different scales. High pass filters are used to analyze the high frequencies, and low pass filters are used to analyze the low frequencies.

The resolution of the signal, which is a measure of the amount of detail information in the signal, is changed by the filtering operations, and the scale is changed by upsampling and downsampling (subsampling) operations [24].

Subsampling a signal corresponds to reducing the sampling rate, or removing some of the samples of the signal. Subsampling by a factor n reduces the number of samples in the signal n times.
Upsampling a signal corresponds to increasing the sampling rate of a signal by adding new samples to the signal. Upsampling a signal by a factor of *n* increases the number of samples in the signal by a factor of n.
DWT employs two sets of functions, called scaling functions and wavelet functions, which are associated with low pass and high pass filters, respectively. The decomposition of the signal into different frequency bands is simply obtained by successive high pass and low pass filtering of the time domain signal.
Two sets of coefficients are computed: approximation coefficients CA_1, and detail coefficients CD_1. These vectors are obtained by convolving $x[n]$ with the low pass filter for approximation and with the high pass filter for detail.
The procedure starts with passing the signal $x[n]$ through a half band digital low pass filter with impulse response h[n]. Filtering corresponds to convolution of the signal with the impulse response of the filter. The convolution operation in discrete time is defined as follows [24]:

$$x[n] * h[n] = \sum_{k=-\infty}^{\infty} x[k].h[n-k] \tag{3.9}$$

A half band low pass (HBLP) filter g[n] removes all frequencies that are above half of the highest frequency in the signal.
After passing the signal through a HBLP filter, half of the samples can be eliminated, since the highest frequency of the signal becomes $\frac{\pi}{2}$ radians instead of π radians. Simply discarding every other sample will subsample the signal by two, and the signal will then have half the number of points. The scale of the signal is then doubled. Only the subsampling process changes the scale. Half band low pass filter h[n] removes half of the frequencies, which can be interpreted as losing half of the information.
This procedure can mathematically be expressed as:

$$y_{high}[k] = \sum_{n} x[n].g[2k-n] \tag{3.10}$$

$$y_{low}[k] = \sum_{n} x[n].h[2k-n] \tag{3.11}$$

Where $y_{high}[k]$ and $y_{low}[k]$are the outputs of the highpass and lowpass filters, respectively, after subsampling by 2.

Only half the number of samples characterizes the entire signal, so, the decomposition halves the time resolution. In the other hand, frequency resolution will be doubled since the frequency band of the signal spans only half the previous frequency band.

The same procedure is maintained for further decomposition. At every level, the filtering and subsampling will result in half the number of samples and hence half the time resolution, also half the frequency band spanned and hence double the frequency resolution. Figure 3.2 illustrates this procedure, where x[n] is the original signal to be decomposed, and h[n] and g[n] are low pass and high pass filters, respectively. The bandwidth of the signal at every level is marked on the figure as "f"[25].

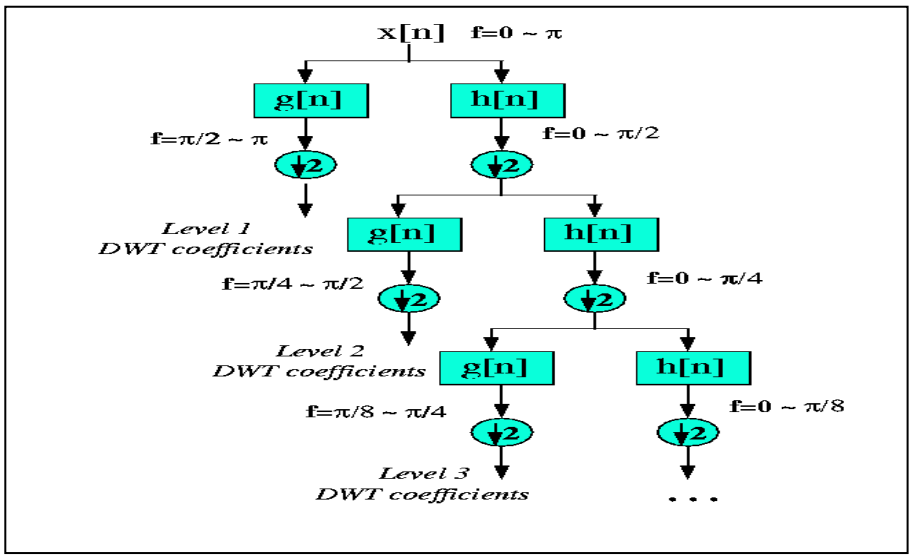

Figure 3.2: Signal decomposition into three levels using LPF and HPF [25]

The prominent frequencies of the original signal appear as high amplitudes in the region of the DWT signal that includes those particular frequencies. If the main information of the signal lies in the high frequencies, the time localization of these frequencies will be more precise, since they are characterized by more number of samples. If the main information lies only at very low frequencies, the time localization will not be very precise, since few samples are used to express signal at these frequencies. This procedure offers a good time resolution at high frequencies, and good frequency resolution at low frequencies. [26]

There are many DWT families, one of the most commonly used set is that formulated by the Belgian mathematician Ingrid Daubechies in 1988. Based on recurrence to generate finer discrete samplings of an implicit mother wavelet function; each resolution is twice that of the previous scale [27].

The Daubechies wavelet transforms are defined by computing running averages and differences via scalar products with scaling signals and wavelets.

There are many Daubechies transforms. The most used one is the Db4 wavelet transform.
Mathematically it is defined as follows:

If a signal x has an even number N of values, then the 1-level Db4 transform is the mapping $x \overset{D_1}{\rightarrow} (a^1|d^1)$ from the signal x to its first trend subsignal a^1 and first fluctuation subsignal d^1.

Each value a_m of $a^1 = (a_1, \dots, a_{N/2})$ is equal to a scalar product: $a_m = x.V_m^1$ of x with a 1-level scaling signal V_m^1. Likewise, each value d_m of $d^1 = (d_1, \dots, d_{N/2})$ is equal to a scalar product: $d_m = f.W_m^1$ of x with a 1-level wavelet W_m^1.

The Db4 wavelet transform can be extended to multiple levels as many times as the signal length can be divided by 2.

Likewise, the definition of a k-level Db4 transform is obtained by applying the 1-level transform to the preceding level trend subsignal, and the values of the k-level trend subsignal a^k and fluctuation subsignal d^k are obtained as scalar products of the signal with k-level scaling signals and wavelets.

The function $\psi(t)$ represents high frequency parts of the signal and $\Phi(t)$ represents smooth and low frequency parts of the signal. Discrete Wavelet Transform has number of advantages when applied for ECG analysis. ECG feature extraction is preceded by a band pass filter to suppress the P and T waves and noises before sending the signal for characteristic detection.

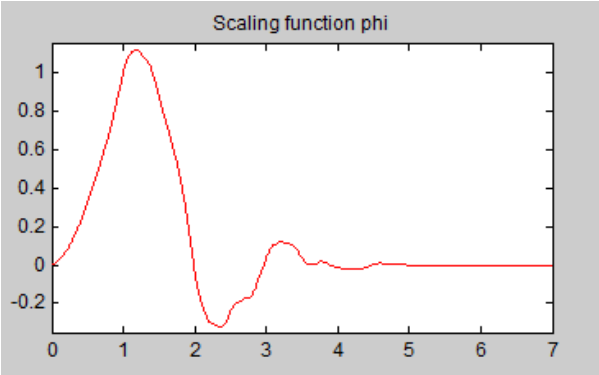

Figure3.3:Wavelet scaling function

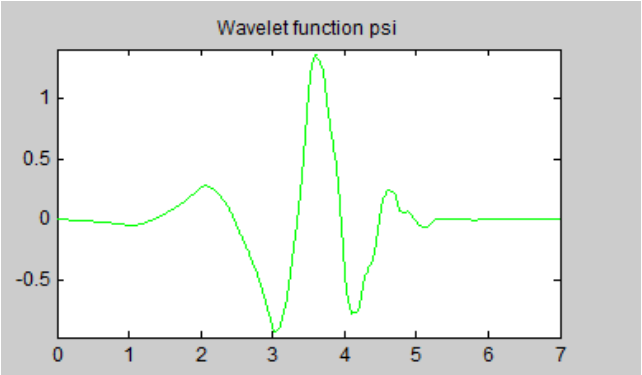

Figure3.4:Wavelet function

Many data operations can now be done by processing the corresponding wavelet coefficients. For instance, one can do data smoothing by thresholding the wavelet coefficients.

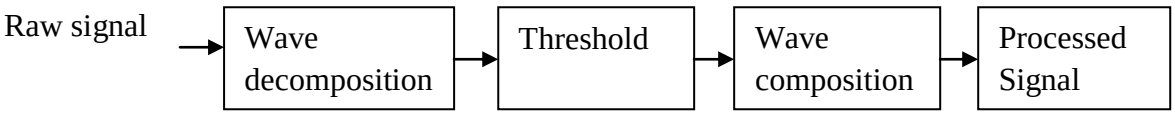

Figure3.5: Signal analysis using wavelets.

Conclusion:

In this chapter, we have introduced three mostly used algorithms for ECG signal analysis and peaks identification:

- Pan& Tompkins: Based on the use of band pass filters, processes in time domain.
- FFT: Based on the decomposition of the signal for eliminating the lower frequencies, used in frequency domain.
- Wavelet algorithm: based on the use of the band pass filters. It processes in both time domain and frequency domain.

Introduction

This chapter deals with the practical section. It focuses on processing ECG signal based on two developped algorithms which are Pan& Tompkins and FFT using two databases: the first one is the benchmark MIT dataset, the second is developped in collaaboration with a reseacher from CDTA.

4.1 Hardware description

4.1.1 Electrodes and patches

Electrodes used to record the ECG voltages are placed on the human body with the patches. It is composed of small metal which is able to catch low amplitude voltages(0.05mV to 10mV), very high input impedance, and low current input level.

Figure 4.1: The electrodes

Figure4.2: The patches

4.1.2 Shimmer device

Shimmer is an open flexible sensor platform intended for qualified personal conducting research.

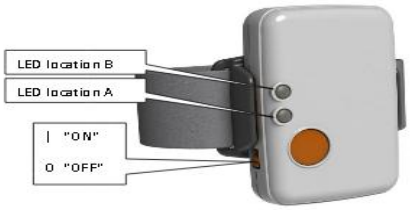

Figure 4.3: Shimmer3 hardware

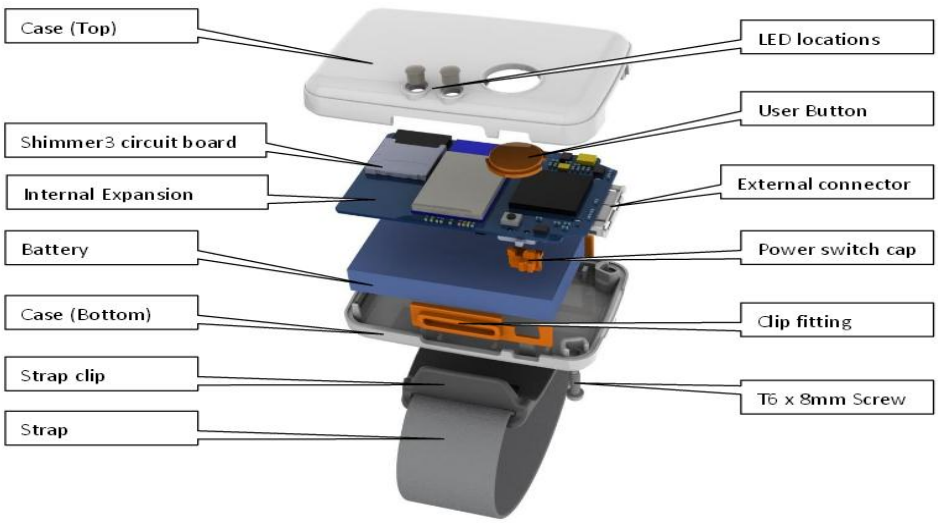

Figure 4.4: Shimmer3 exploded view

4.1.2.1 Pairing a shimmer

In order to capture data from a shimmer sensor using Bluetooth connection, this later must first be set up in a process called pairing.

4.1.2.2 Setting up a shimmer data stream

Shimmer 'connect' is a host side application used to configure a single shimmer and stream data from it. To run the shimmer connect application, we just double click on the application executable.

We need then to use the select COM Port drop down menu to select the correct COM port number for our shimmer(Figure 4.5). Then we choose name and activity(Figure 4.6):

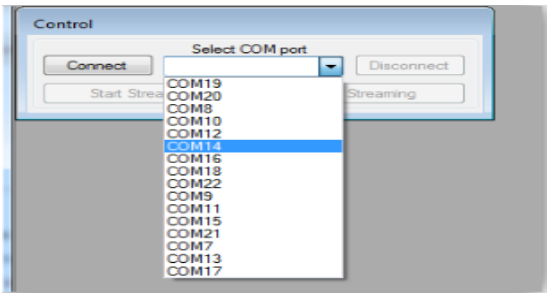

Figure4.5: Selecting COM port in Shimmer Connect

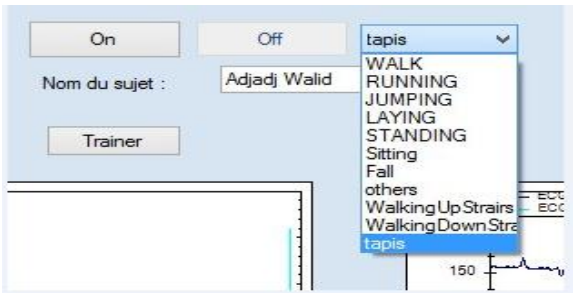

Figure4.6: Entering name and activity

4.1.2.3 Connect to a Shimmer

After ensuring the Shimmer unit is powered, the Connect button is pressed on the Shimmer Connect application to establish a bluetooth connection between the Shimmer and the host side machine.

4.1.2.4 Stream from the Shimmer

To strat the Shimmer streaming data to the Shimmer Connect application, we press the Streaming button.

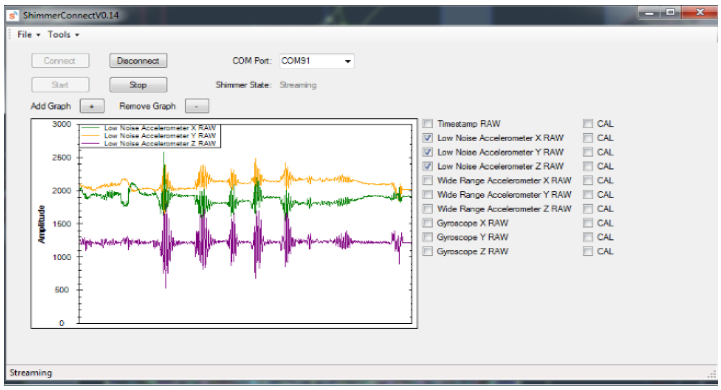

Figure 4.7:Shimmer streaming data

Data can be stored to CSV file by pressing Tools→Save to CSV. To stop transmission, we press the Stop Streaming button. To release the connection to the host application and remain idle, we press Disconnect.

4.1.3 ECG datasets

4.1.3.1 MIT-BIH arrhythmia database

From all the available ECG database in Physiobank, we have selected the MIT-BIH arrhythmia database, because it contains a large variety of ECGs, including signals, which are rarely observed but clinically important.

The difference with other databases is that it focusses on heartbeat positions with different QRS morphologies, while others foccus on other waves such as P, T or other features such as ST segments, rhythm changes, and signal quality changes.

The MIT-BIH arrhythmia database contains 48 ECG recordings each of 30 minutes length and two channel ambulatory ECG recordings. Every record contains three files with different suffixes that indicate their content:

- **.dat** (signal) file: a binary file containing the digitized samples of the ECG signal.
- **.hea** (header) file: a short text file describing the signal features.
- **.atr** (annotations) file: it contains labels, each of which describes signal features at specific time, such as QRS complex location, and type.

The sampling frequency is 360Hz and the total number of samples in each record is 650000 samples.

Two cardiologists have annotated all beats and calculated the total number of R peaks for each record. The corresponding results are used in our work to evaluate the performance of our program.

4.1.3.2 Recorded database

This dataset was acquired in collaboration with a qualified staff from CDTA. Each record represents three minutes ECG signal taken during activity of the person under consideration. The total number of persons used in our experiment is 12 persons. The dataset was acquired used the Shimmer hardware described above. The sampling frequency of the Shimmer device is 125 Hz. The electrodes placement is shown in the Figure4.8 below:

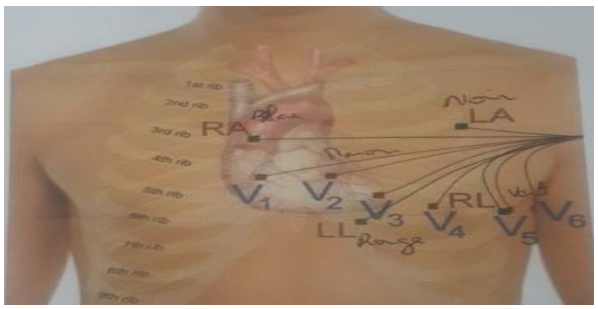

Figure4.8: Electrodes positions for ECG measurement [27]

Five electrodes are used: LA (Left Arm), RA (Right Arm), V_1, LL(Left Leg), RL(Right Leg) and V_6. Following the precordial leads method described in chapter 1, electrodes placement is done by a doctor for each of the 12 volunteers doing the same activity (running while changing the speed each 30 second for each record).

Our goal is to record a raw ECG signal considering two states: rest and activity. The activity consists of running with different speeds on a roller tape. As we have mentioned, each record is about 3 minutes length. It is divided into sub intervals each one is of 30 seconds length.

As a first phase, the person stays at rest on a roller tape for 30 seconds. Then, for the next 30seconds, the speed is adjusted to the value 3 indicated on the roller tape. After that, the speed is doubled for the same duration (30seconds), it is then decreased to 3 for other 30 seconds. After that, the speed is doubled another time for 30 seconds. As a last phase, the speed is decreased and the person comes back to its original state (comes to rest).

4.1.4 Simulation and results

In the following, we show the steps and results of our simulations:

4.1.4.1 Results of simulation of Pan & Tompkins program using MIT-BIH database

The results of our simulation over a record of the MIT-BIH database are shown below:

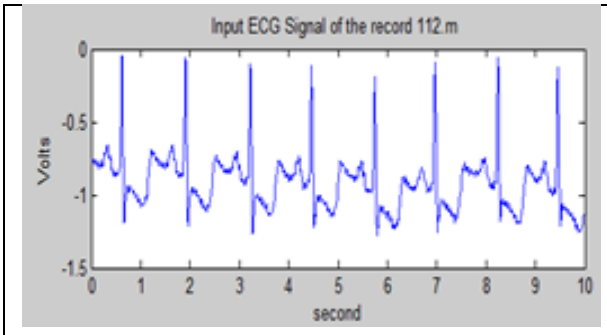

Figure 4.9: Raw ECG input

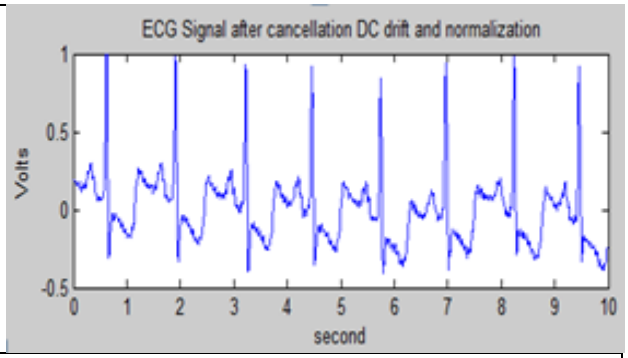

Figure4.10: DC drift Elimination and normalization

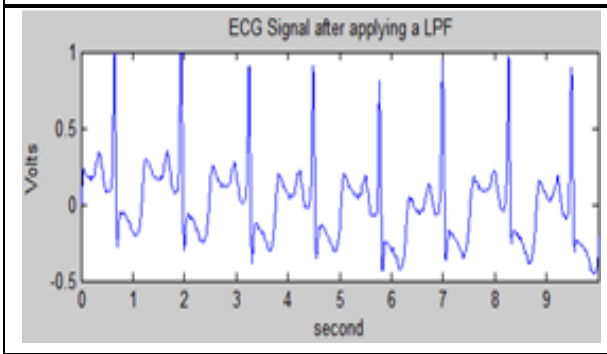

Figure4.11: LPF application

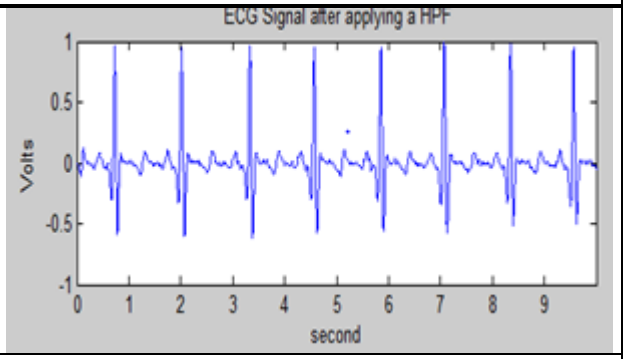

Figure4.12: HPF application

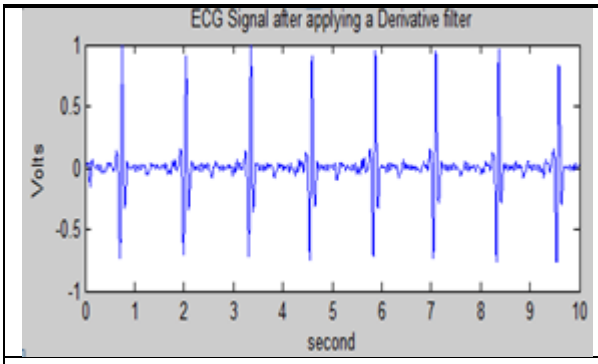

Figure4.13: Derivative filter application

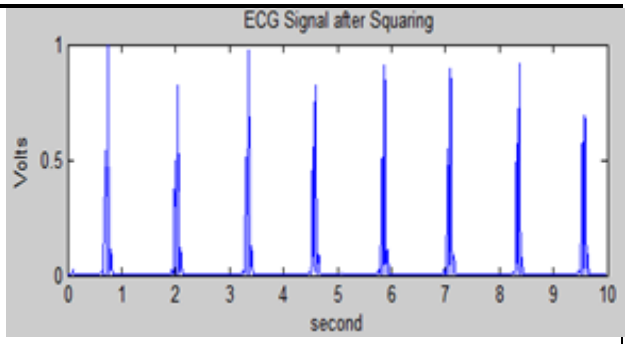

Figure4.14: Squaring function

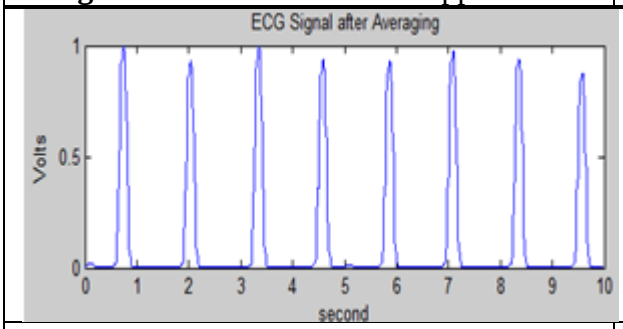

Figure4.15: Averaging

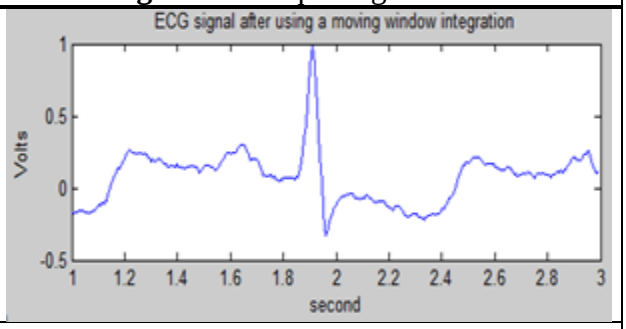

Figure4.16: moving window integration

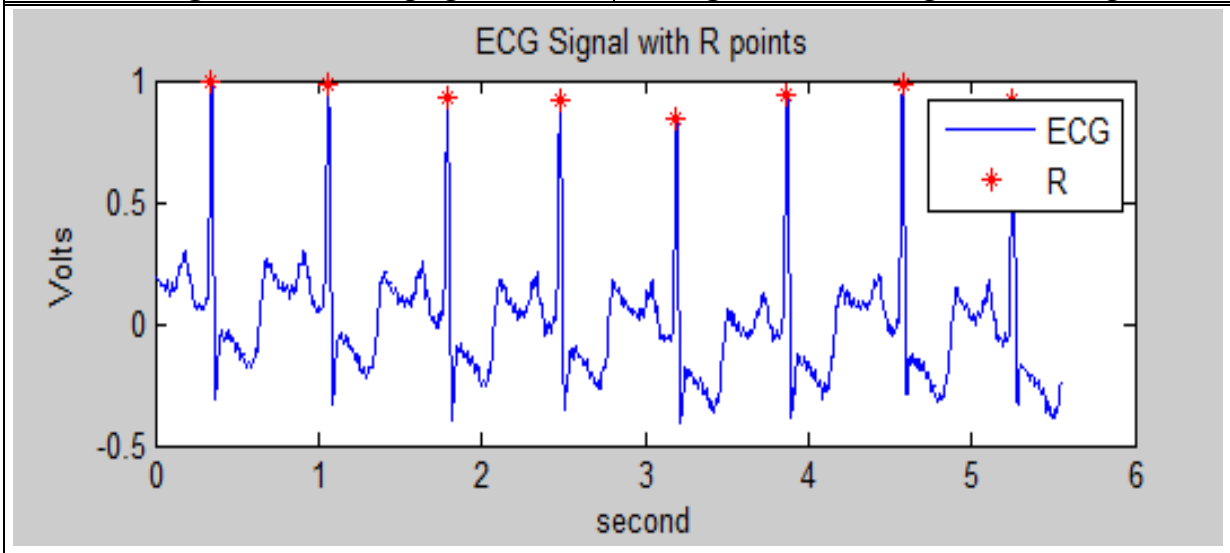

Figure4.17: QRS complex detection

Hence, the number of QRS complexes can be obtained from this detection; the program will count up each time an R peak is detected. The results for the same record are shown in Figure 4.18 below. Taking into consideration all the samples with a total of 650000 samples and a sampling frequency of 360Hz:

```
\n$> LOADING DATA FINISHED

NbrOfRPeaks =

        2545
```

Figure4.18: Detection of the number of R peaks

4.1.4.2 Results of simulation of FFT program using MIT-BIH database

The FFT basic is to remove first lower frequencies, than go through the step of peak detection.

After simulating the FFT program for the record 100.m, the results are shown in Figure 4.19 below:

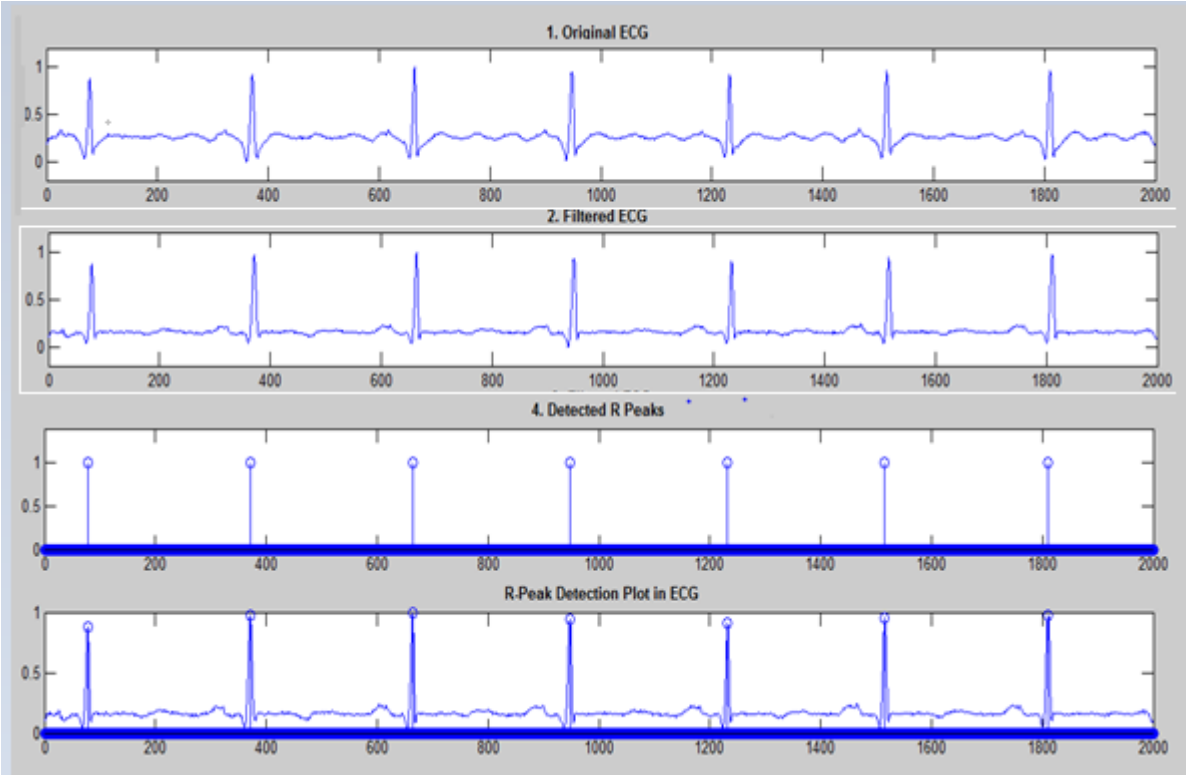

Figure 4.19: Result of simulating FFT program for MIT-BIH database record 100.m

For all the 48 records contained in the MIT-BIH database, we have simulated and run the two programs: Pan & Tompkins and FFT. We have then computed the error for each one and also for the whole database.

Our results are shown in Table 4.1 which follows:

Table4.1: Results of evaluating the two algorithms using the MIT-BIH data base.

patient	MIT (beats)	Pan method results(beats)	False detection (beats)	Error %	FFT method results(beats)	False detection (beats)	Error %
100	2273	2272	1	0.04	2273	0	0
101	1865	1871	6	0.32	1864	1	0.05
102	2187	2199	12	0.55	2186	1	0.05
103	2084	2083	1	0.048	2084	0	0
104	2229	2226	3	0.13	2320	91	4.08
105	2572	2687	115	4.47	2623	51	1.98
106	2027	1973	54	2.66	1851	176	8.68
107	2137	2121	16	0.75	2382	245	11.46
108	1774	1920	146	8.23	1405	369	20.8
109	2532	2527	5	0.2	2509	23	0.9
111	2124	2127	3	0.14	2121	3	0.14
112	2539	2545	6	0.24	2548	9	0.35
113	1795	1794	1	0.06	1795	0	0
114	1879	1888	9	0.48	1336	543	28.9
115	1953	1953	0	0	1953	0	0
116	2412	2395	17	0.7	2390	22	0.91
117	1535	1537	2	0.13	1539	4	1.56
118	2288	2312	24	1.05	2371	83	3.63
119	1987	1992	5	0.25	1983	4	0.2
121	1863	1870	7	0.38	1884	21	1.13
122	2476	2477	1	0.04	2479	3	0.12
123	1518	1518	0	0	1518	0	0
124	1619	1622	3	0.19	1615	4	0.25
200	2601	2598	3	0.12	2716	115	4.42
201	2000	1945	55	2.75	1895	105	5.25
202	2136	2133	3	0.14	2122	14	0.66
203	2980	3040	60	2.01	2756	224	7.51
205	2656	2663	7	0.26	2667	11	0.41
207	2332	2185	147	6.30	3073	741	31.78
208	2955	2916	39	1.32	2060	895	30.29
209	3005	3010	5	0.17	3023	18	0.6
210	2650	2640	10	0.38	2387	263	9.92
212	2748	2751	3	0.11	2749	1	0.04
213	3251	3337	86	2.65	3242	9	0.28
214	2262	2263	1	0.04	2267	5	0.22
215	3363	3363	0	0	3365	2	0.06
217	2208	2201	7	0.32	2247	39	1.77
219	2287	2152	135	5.9	2152	135	5.90
220	2048	2048	0	0	2048	0	0
221	2427	2421	6	0.25	2345	82	3.38
222	2483	2505	22	0.89	2392	91	3.66
223	2605	2599	6	0.23	2564	41	1.57
228	2053	2214	161	7.84	2072	19	0.93
230	2256	2258	2	0.09	2260	4	0.18
231	1573	1571	2	0.13	1571	2	0.13
232	1780	1788	8	0.45	1777	3	0.17
233	3079	3078	1	0.03	3554	475	15.43
234	2753	2748	5	0.2	2750	3	0.11
total	**110123**	**110333**	**1201**	**1.09%**	**109083**	**4950**	**4.49%**

4.1.4.3 MIT-BIH simulation results discussion

Table 4.1 above, summarizes the performance of our algorithms using the MIT-BIH data base.

The Pan & Tompkins method produces a total of 1201 false detected beats. This leads to a detection failure of 1.09%.

The FFT method produces 4950 false detected beats for a total of 4.49% detection error.

These errors are mainly caused by the ECG signal contaminations (noise, artifacts and baseline drifts), also due to the waves morphology because the ECG recordings belong to patients suffering from cardiovascular arrhythmia.

As an example, the worst case detection failure for Pan Method is encountered for records 228, 207 and 108.Whereas, for the FFT method it appears in records 207, 208 and 233. These records have the greatest false detection rates due to the characteristics of their waves. In particular, the P wave is characterized by high amplitude and peaked morphology hence it is confused to be an R peak rather than a P wave which gives rise to the high detection error.

4.1.4.4 Results of simulation of Pan &Tompkins program using our recorded database

The results of simulation on our recorded database (for record 1) are shown in the following page.

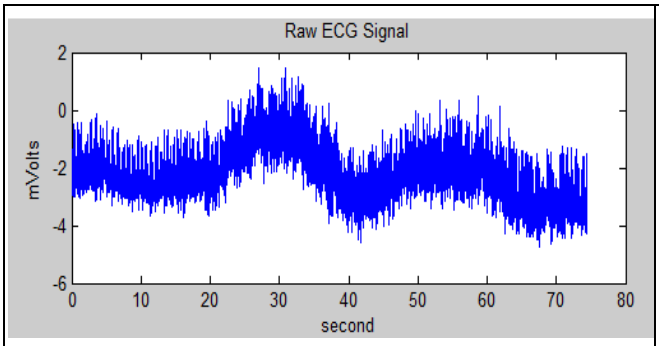

Figure 4.20: Raw ECG signal

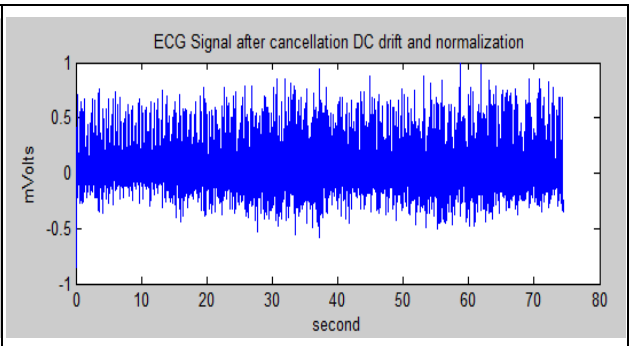

Figure4.21: DC drift Elimination and normalization

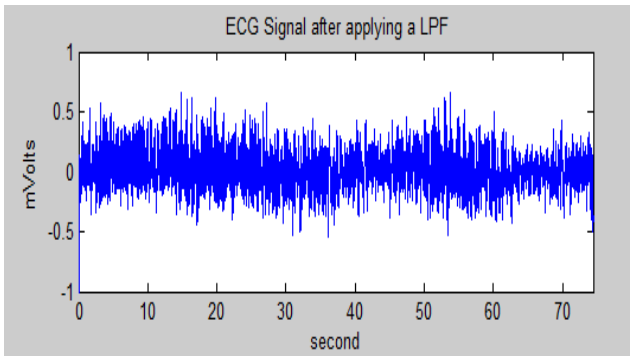

Figure4.22: LPF application

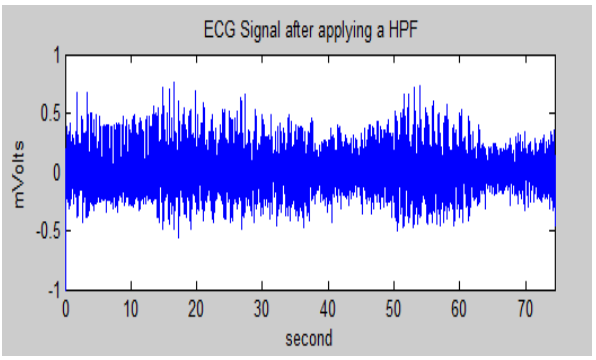

Figure4.23: HPF application

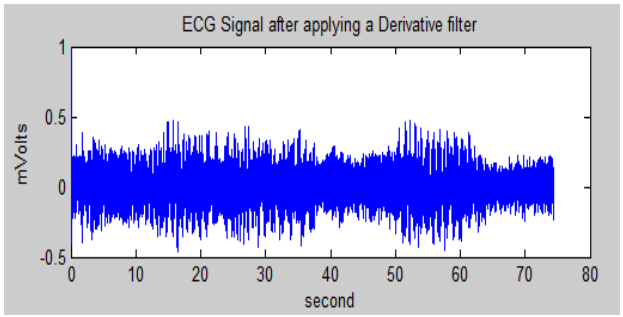

Figure4.24: Derivative filter application

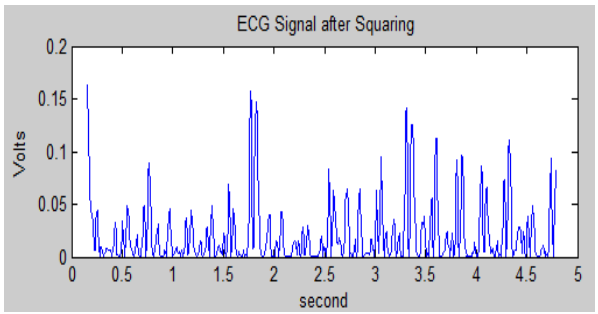

Figure4.25: Squaring function

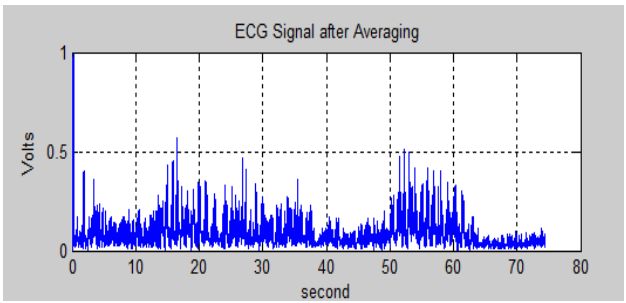

Figure4.26: Averaging

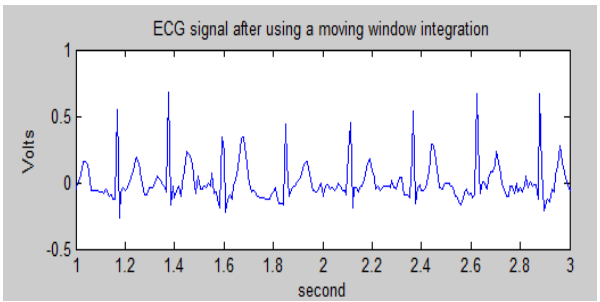

Figure4.27: moving window integration

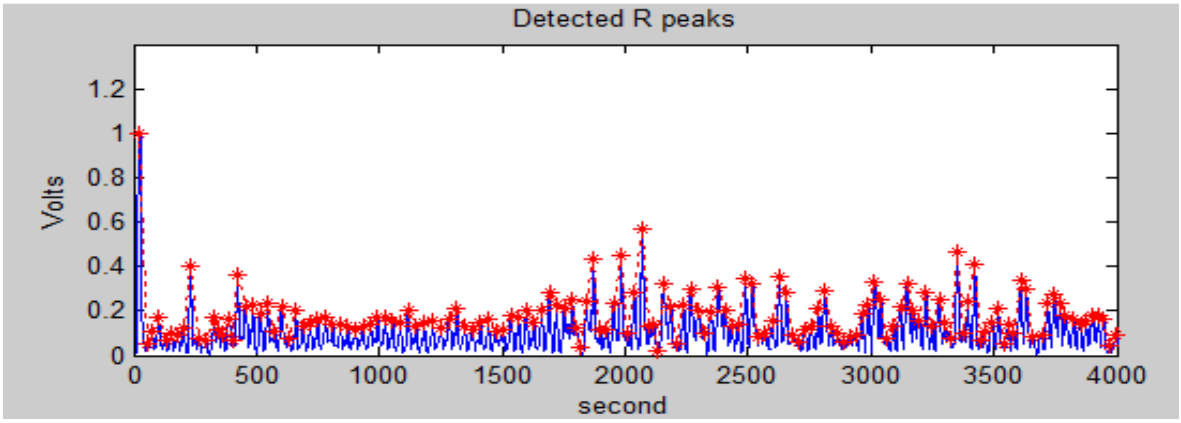

Figure 4.28: R peak detection plot

Hence, the number of R peaks can be obtained from this detection. The results for the same record (record 1) are shown in Figure 4.29 below. The sampling frequency is 125Hz.

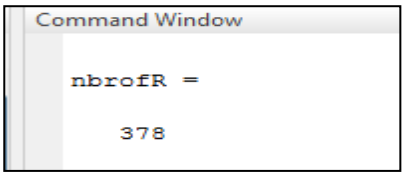

Figure 4.29: The number of R peaks for the record number 1

4.1.4.5 Results of simulation of FFT program using recoded database

After simulating the FFT program for the record number 1, the results are shown in Figure 4.30 below:

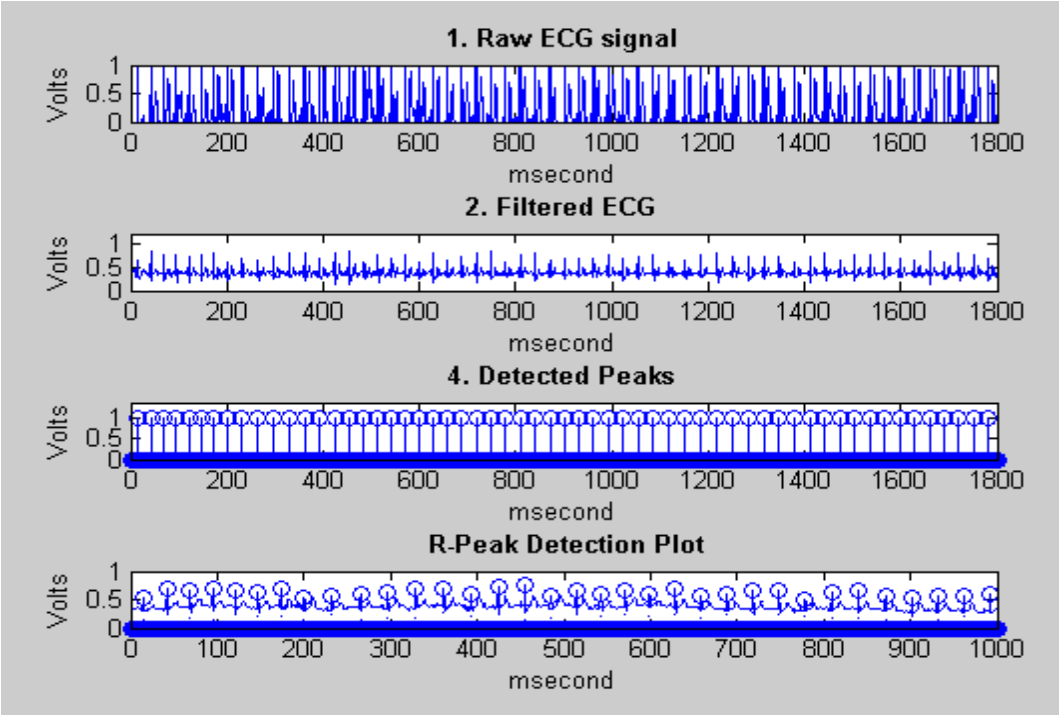

Figure 4.30: Results of simulating FFT program over recorded data base (record 1)

The same procedures are applied for each of the 12 ECG records. The results are shown in Table4.2

Table4.2: Results of evaluating the two algorithms using our recorded data base.

	Name	Doctor counting	P&T Algo.	False Detection (beats)	Error (%)	FFT algo.	False detection (beats)	Error (%)
1	Abderrahmane	378	378	0	0	375	3	0.79
2	Benziadi	463	460	3	0.65	458	5	1.07
3	Hakim	325	365	40	12.3	323	2	0.61
4	Houcine	447	442	5	1.19	402	45	10.06
5	Houcine2	351	361	10	2.49	347	4	1.14
6	Nassim	439	436	3	0.68	437	2	0.45
7	Nadjet	425	422	3	0.7	424	1	0.23
8	Oussama	316	327	11	3.48	316	0	0
9	Rachid	458	453	5	1.09	449	9	1.96
10	Ratiba	363	363	0	0	357	6	1.65
11	Tahar	279	296	17	6.09	281	2	0.72
12	Walid	360	360	0	0	320	40	11.11
	Total	4604	4663	97	2.11%	4589	119	2.58%

The above results summarize the performance of the two methods (Pan & Tompkins and FFT).

- The Pan & Tompkins method simulation resulted in 97 false detections over a total of 4604 beats. This produces an error of 2.11%.
- On the other hand, FFT method produced 119 false detections which is equivalent to an error rate of 2.58%.

The false detections of the two methods may be due to the recording circumstances. The data acquisition has been recorded while the persons were on activity (running on rolling tape with different speeds). As a matter of fact, the movement of the persons during the recording phase increases the heart rate. Also the electrodes move, hence, a relative increase of the noise level is encountered.

4.1.5 Results discussion

The Pan &Tompkins method simulated for both MIT-BIH database and recorded database is of high performance compared to that of FFT as it is noticed from the simulation results. This is mainly noticed while using the MIT-BIH database since this later contains records for patients having cardiovascular problems; hence, they have abnormal ECG characteristics.

We can say that the time domain Pan & Tompkins algorithm outperforms FFT algorithm.

Conclusion

In this chapter we have dealt with two different algorithms:

- The Pan & Tompkins algorithm, used in time domain.
- The FFT algorithm, used in frequency domain.

Even though the two methods are different, their performances are comparable.

QRS detection has been a hot research topic for long time ago; however, nowadays the main concern is the performance not the rate of detection.

The two algorithms were implemented using MATLAB and tested over two sets of database: the MIT-BIH database and the recorded database.

Our dataset was recorded using a hardware which is a Shimmer device and platform described earlier in this chapter. The records are made and then saved into Excel files. These files are used in MATLAB to load the desired database.

General conclusion

Analysis of the heart electrical activity is relevant to detect cardiovascular diseases. The ECG signal is a repetitive waveform that comprises several waves distinguished each other by frequencies and amplitudes. These waves originate from the heart electrical activity.

In conventional methods of ECG diagnosis, the goal is to find whether the ECG signal is different from normal sinus rhythm in terms of the morphology of each component, time interval and heart rate. The ECG has a magnitude of only few mV. It is usually contaminated with several types of noise. Moreover, the measurement conditions are relatively complicated. Therefore, the pretreatment of ECG is a basis of accurate ECG analysis.

In this project, we have implemented two QRS detection algorithms using MATLAB, the first one which is a purely time domain-based implementation of Pan &Tompkins algorithm, the second one was a frequency domain implementation of FFT algorithm.

A good filtering technique is the one that cancels the noise without trailing important signal information to get a denoised ECG signal used later on for further analysis. For our ECG preprocessing steps, we have used both FIR and IIR digital filters. For each step, the type of the noise present is first depicted, then filter characteristics are designed. Our goal from these steps was to get a denoised ECG signal that is then, processed for the QRS detection.

We have assessed the two methods on two different datasets, the first one has been acquired from people at rest, the second one was acquired from people during activity.

We have recorded our data base using a very sophisticated hardware available in CDTA, this data base was registered in some special conditions at rest and while doing an activity for different persons. Then stored and loaded so as to be used for further analysis.

The two methods give very good results especially the Pan & Tompkin method which gave a relatively small error of 1.09% compared to the FFT program which produces an error of 4.99% when tested over the MIT-BIH data base.Whereas, when tested over our data base, the detection failure is 2.11% for the Pan&Tompkin program and 2.58% for the FFT program.

These errors for both cases were relatively small, hence, we can say that our results are satisfactory. We may conclude that the aim of our project was successfully reached. The achieved results indicate that the two algorithms can help cardiologists in the diagnosis of various types of arrhythmia. These algorithms can be used to support diagnosis decisions made using other clinical tests and investigations, and help to proceed to the following ECG analysis step (e.g. classification).

Suggestions:

As an expansion of this project, we propose to enhance the implemented algorithms trying to reduce their failures and decrease the execution time. This will give better performance and accurate results. Furthermore, the data base could be recorded in a certain way to potentially take into consideration different cardiac rhythms (stress, jumping…etc), this will need to reconsider all the preprocessing steps to fit in the best criteria for a good detection performance.

General conclusion

List of acronymes

QRS	Complex QRS
ECG	Electrocardiogram
MIT	Massashuset Institute of Technology
BIH	Beth Israel Hospital
AV	Atrioventricular node
VL	Left arm potential
VR	Right Arm potential
VF	Left Leg potential
aVL	Left Arm Augmented Lead
aVR	Right Arm Augmented lead
aVF	Left Leg Augmented lead
LA	Left Arm
RA	Right Arm
LL	Left Leg
RL	Right Leg
SA	Sinus Atrioventricular node
Bpm	Beat Per Minute
EMG	Electromyograms
IIR	Infinite Impulse Response
FIR	Finite Impluse Response
DSP	Digital Signal Processing
ADC	Analog to Digital Converter
DAC	Digital to Analog Converter
DE	Difference Equations

List of acronymes

DTFT	Discrete Time Fourier Transform
LHP	Left Half Plane
RHP	Right Half Plane
MA	Moving Average
FFT	Fast Fourier Transform
DWT	Discrete Wavelet Transform
HBLP	Half Band Low Pass filter
Db4	Daubechies order 4
LPF	Low Pass Filter
HPF	High Pass Filter
CDTA	Centre de Developpement des Technologies Avancées

List of figures

Figure 1.1 : Basic heart anatomy schema 02

Figure 1.2: Conduction system of the heart consists of Sinus node,..... 03
Atrioventricular node, Bundle of His, bundle branches and Purkinje fibers

Figure 1.3 Schematic representation of ECG waveform generation by 04
summing of different action potentials

Figure 1.4: Einthoven triangle electrodes placements for limb derivation 05

Figure 1.5: Goldberger electrodes placements for augmented limb leads 06

Figure 1.6: Schematic representation of augmented limb leads calculation 06

Figure 1.7 : Precordial leads electrodes positions 07

Figure1. 8: Normal ECG waveform 07

Figure 1.9: ECG signal pretreatement and feature data extraction system chart 09

Figure 2.1: Digital Filter Stages 11

Figure 2.2: (a): Low-pass filter, (b) Band-pass filter, (c) High-pass filter (d) Band reject filter..... 12

Figure 2.3: The logical structure of an FIR filter. 12

Figure 2.4: Realistic versus Ideal Filter Response 13

Figure 2.5: Impulse responses of FIR and IIR filters 14

Figure 2.6: A structure of an FIR filter 15

Figure2.7: Block diagram of an IIR filter 18

Figure3.1: Block diagram of Pan & Tompkins algorithm..... 24

Figure 3.2: Signal Decomposition Into Three Levels Using LPF And HPF 29

Figure 3.3: Wavelet scaling function 30

Figure 3.4:Wavelet function..... 30

Figure3.5: Signal Analysis Using Wavelets. 30

Figure 4.1: The electrodes..... 31

Figure4.2: The patches 31

Figure 4.3: Shimmer3 hardware 31

Figure 4.4 : Shimmer3 exploded view 31

Figure4.5: Selecting COM port in Shimmer Connect 32

Figure4.6: Entering name and activity..... 32

Figure 4.7:Shimmer streaming data 32

Figure4.8: Electrodes positions for ECG measurement 33

List of figures

Figure 4.9: Raw ECG input 34

Figure4.10: DC drift Elimination and normalization 34

Figure4.11: LPF application 34

Figure4.12: HPF application 34

Figure4.13: Derivative filter application 35

Figure4.14: Squaring function 35

Figure4.15: Averaging 35

Figure4.16: moving window integration 35

Figure4.17: QRS complex detection 35

Figure4.18: Detection of the number of R peaks 35

Figure 4.19: Result of simulating FFT program for MIT-BIH database record 100.m 36

Figure 4.20: Raw ECG signal 39

Figure4.21: DC drift Elimination and normalization 39

Figure4.22: LPF application 39

Figure4.23: HPF application 39

Figure4.24: Derivative filter application 39

Figure4.25: Squaring function 39

Figure4.26: Averaging 39

Figure4.27: moving window integration 39

Figure4.28: R peak detection plot 40

Figure 4.29: The number of R peaks for the record number 1 40

Figure 4.30: Results of simulating FFT program over recorded data base (record 1) 40

List of tables

Table4.1: Results of evaluating the two algorithms using the MIT-BIH data base..... 37

Table4.2: Results of evaluating the two algorithms using our recorded data base. 41

References

[1]L.Sornmo and P.Laguna,"Bioelectrical Signal Processing in Cardiac and Neurological Applications." Elsevier Academic Press, June 2005.

[2] Kohler BU, Hennig C, Orlgmeister R. "The principles of software QRS detection". IEEE Eng Med Biol Mag. 2002;21(1):42–57

[3] Jakub Kuzilek," Independent Component Analysis: Applications in ECG signal Processing", Department of Cybernetics Faculty of Electrical Engineering Czech Technical University in Prague, 2013.

[4] J. Malmivuo and R. Plonsey, "Bioelectromagnetism: Principles and Applications of Bioelectric and Biomagnetic Fields". Oxford University Press, USA, 1 ed. July 1995.

[5] Bishweshwar Pratap Tasa, Pompy Das and Avinash Sinha, "Simulation Based R-peak and QRS detection in ECG Signal", Current Trends in Technology and Science,DBCET, Azara, Guwahati. ISSN:2279-0535, Volume :2, Issue:4

[6] W. Eithoven, "Weiteres uber das Elektrokardiogramm", Pfugers Archiv-european Journal of Physiology, vol.122, pp, 517-584, 1908, 27

[7] Dr. BENALI Radhwane, "Analyse du signal ECG par réseau adaptif d'ondelettes en vue de la reconnaissance de pathologies cardiaques", Pages 27-33, year 2013.

[8] Kiran Kumar Jembula, Prof. G. Srinivasulu, Dr. Prasad K.S, "Design of Electrocardiogram System on FPGA" International Journal Of Engineering And Science Vol., Issue 2 (May 2013), PP2127.

[9] Josef dubovy,"biomedical electronics", 1978

[10]http://www.merckmanuals.commediaprofessionalfiguresCVS_ECG_waves.gif Generation and recording of ECG

[11]: Lina Zhang, "The Pretreatment and Feature Data Extraction of ECG Based on Matlab". Normal University Hohhot, China

[12] G. M. Friesen, T. C. Jannett, M. A. Jadallah, S. L. Yates, S. R. Quint, and H. T. Nagle, "A Comparison of the Noise Sensitivity of Nine QRS Detection Algorithms," *IEEE Transactions on Biomedical Engineering,* 37, pp. 85-98, 1990.

[13] Der YZ, Saki MC, Gcer HA. "Removal of power line interference in signal-Averaged electrocardiography systems", IEEE Trans Biomed Eng. 1995 Jul; 42(7):731-5

[14] Ajay Bharadwaj and Umanath Kamath," Cypress Semiconductor Corp", 2/14/2011

[15]C. S. Weaver, et al.,"Digital Filtering with Applications to Electrocardiogram Processing," IEEE Transactions on Audio and Electroacoustics, Vol. Au-16, No. 3, pp. 350-391, September 1968.

[16]C. D. McManus, K. D. Neubert, and E. Cramer, "Characterization and Elimination of AC Noise in Electrocardiograms: A Comparison of digital Filtering Methods," Computer Biomedical Res., 26, pp. 48–67, 1993.

References

[17] Yatindra Kumar and Gorav Kumar Malik, ”Performance Analysis of different Filters for Power Line Interface Reduction in ECG signal ” , International Journal of Applications(0975-8887). June 2010.

[18]Dr. Konstantinos Tatas, “Real-time Digital Signal Processing with the TMS320C6x”.

[19] Dr. Daamouche DSP courses. 2015/2016

[20] John Wiley & Sons, INC, “Biomedical Signal Analysis a Case Study Approach”, IEEE Press, Rangaraj M. Rangayyan, 2005.

[21]Pan J., and TOMPKINS W.J. “A Real Time QRS Detection Algorithm ”, IEEE Trans. Biomed. Eng., 32, pp.230-236. 1985

[22]O. Pahlm and L. Sornmo, “Software QRS Detection in Ambulatory monitoring—a review”, Medical and Biological Engineering and Computing, vol.22, no.4, pp. 289-297, 1984.

[23] S. Sumathi, Dr. M. Y. Sanavullah, “Comparative Study of QRS Complex Detection in ECG Based on Discrete Wavelet Transform”, International Journal of Recent Trends in Engineering, vol 2, No.5, Engineering College, Salem, India. November 2009.

[24] Ingrid Daubechies, “Ten Lectures on Wavelets”, Society for Industrial and Applied Mathematics, Rutgers University and AT&T Bell Laboratories Philadelphia, Pennsylvania.1992

[25] Robi Polikar, “The Wavelet Tutorial Part IV”, Multiresolution Analysis: The Discrete Wavelet Transform.

[26] I. Daubechies,Ten Lectures on Wavelets. Philadelphia, PA, USA: Society for Industrial and Applied Mathematics, 1992.

[27] Shimmer user manual Rev3g.2014